Paula Christina Mattos dos Santos

ENCAPSULATION OF SUPERPARAMAGNETIC NANOPARTICLES AND 4-NITROCHALCONE IN POLY(THIOETHER-ESTER) FOR BIOMEDICAL APPLICATIONS

Florianópolis
2018

Ficha de identificação da obra elaborada pelo autor através do Programa de Geração Automática da Biblioteca Universitária da UFSC.

Encapsulation of Superparamagnetic Nanoparticles and 4-Nitrochalcone in Poly(thioether-ester) for Biomedical Applications

por

Paula Christina Mattos dos Santos

Dissertação julgada para obtenção do título de **Mestre em Engenharia Química**, na área de Concentração de **Desenvolvimento de Processos Químicos e Biotecnológicos** e aprovada em sua forma final pelo Programa de Pós-graduação em Engenharia Química da Universidade Federal de Santa Catarina.

Prof. Dr. Pedro Henrique Hermes de Araújo
orientador

Prof.ª Dr.ª Claudia Sayer
coorientadora

Dr. Paulo Emilio Feuser
coorientador

Prof.ª Dr.ª Cíntia Soares
coordenadora

Banca Examinadora:

Prof. Dr. Natan Padoin

Prof. Dr. Acácio Antonio Ferreira Zielinski

Dr.ª Priscilla Barreto Cardoso

Florianópolis, 25 de setembro de 2018.

AGRADECIMENTOS

Gostaria de agradecer a todos que, de alguma forma, contribuíram nestes dois anos de mestrado.

Agradeço ao meu orientador, Prof. Dr. Pedro Henrique Hermes de Araújo, e à minha coorientadora Prof.ª Dr.ª Claudia Sayer, pela oportunidade de participar deste grupo de pesquisa e desenvolver este trabalho, e pela orientação durante estes anos. Ao meu coorientador Dr. Paulo Emilio Feuser, obrigada por compartilhar sua experiência comigo e me guiar na elaboração deste trabalho.

À minha mãe, Neli, pelo apoio, incentivo nas horas difíceis de desânimo e cansaço e pelo amor incondicional. À minha tia, Leonor, minha segunda mãe e grande amiga, por estar sempre presente mesmo de longe e por todo o carinho. Obrigada por sempre acreditarem mais em mim do que eu mesma.

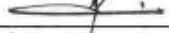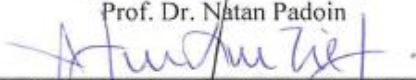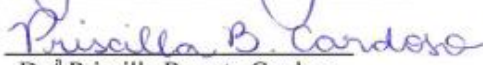Aos colegas do Laboratório de Controle de Processos (LCP), obrigada por toda ajuda que sempre recebi. Obrigada por cada momento de descontração compartilhado durante os cafés, que tonaram nosso dia-a-dia menos pesado. E obrigada por me compreenderem em cada etapa deste trabalho.

Obrigada aos amigos que não compartilham mais o dia-a-dia comigo, mas que estão sempre presentes de muitas outras formas. Ao meu time de flag football, Desterro Atlantis, que me acolheu neste último ano, obrigada por ser meu refúgio, minhas doses diárias de leveza.

Agradeço aos laboratórios e professores que proporcionaram a realização de algumas análises: Laboratório Central de Microscopia Eletrônica (LCME) e Laboratório Interdisciplinar para o Desenvolvimento de Nanoestruturas (LINDEN), ambos da Universidade Federal de Santa Catarina; Prof. Dr. Ricardo Andrez Machado de Ávila, Laboratório de Biologia Celular e Molecular da Universidade do Extremo Sul Catarinense; Prof.ª Dr.ª Maria Eliane Merlin Rocha, Laboratório de Bioquímica e Biologia Celular da Universidade Federal do Paraná; e Prof. Dr. Alexandre Cas Viegas, Laboratório Multiusuário de Difração de Raios X e VSM da Universidade Federal de Santa Catarina.

"You cannot hope to build a better world without improving the individuals. To that end each of us must work for his own improvement, and at the same time share a general responsibility for all humanity, our particular duty being to aid those to whom we think we can be most useful."
(Marie Curie)

RESUMO

O câncer é uma das principais causas de morbidade e mortalidade no mundo, sendo hoje considerado um problema de saúde pública. A maior dificuldade durante o tratamento destas doenças é destruir as células tumorais sem afetar o tecido saudável. As nanopartículas poliméricas magnéticas têm sido consideradas como um sistema eficaz para estes tratamentos, pois contribuem para uma entrega precisa do fármaco, reduzindo os efeitos colaterais e aumentando a eficácia terapêutica. As chalconas são compostos polifenólicos da classe dos flavonóides associados a diversas atividades farmacológicas, cujas propriedades levaram os pesquisadores a considerá-las como potenciais anticarcinogênicos. A polimerização tiol-eno é um novo e promissor campo de estudo devido aos seus atributos, incluindo condições suaves e rápidas taxas de reação sem a formação de subprodutos. Neste trabalho, nanopartículas superparamagnéticas de poli(tioéter-éster) (PTEe) juntamente com o encapsulamento de 4-nitrochalcona (4NC) foram sintetizadas pela primeira vez. A polimerização tiol-eno em miniemulsão foi aplicada usando um monômero α,ω-dieno totalmente renovável obtido a partir do ácido 10-undecenóico e 1,3-propanodiol, ambos derivados do óleo de mamona. Nanopartículas superparamagnéticas foram sintetizadas com sucesso por miniemulsificação e evaporação de solvente, apresentando morfologia esférica, diâmetros em torno de 135 nm e baixos índices de polidispersão. Análises de FT-IR mostraram as bandas de absorção do polímero e das MNPs. Análises de TGA mostraram uma eficiência de encapsulação (EE%) de MNPs maior que 99%. Ensaios de citotoxicidade e microscopia de fluorescência em células HeLa demonstraram que o material não é citotóxico e que, quando exposto a um campo magnético externo, a internalização celular é até três vezes maior. A EE% da 4NC foi maior que 90%. O perfil de liberação de 4NC foi obtido em pH 7,4 e 6,0, utilizando-se uma amostra de MNPs e 4NC encapsuladas simultaneamente. Observou-se que a liberação ocorre por difusão e mais rápida em pH 6,0. As nanopartículas também foram sintetizadas pela polimerização em miniemulsão, que tem a vantagem de incorporar compostos inorgânicos em apenas uma etapa. Características como morfologia, diâmetro e índice de polidispersão não apresentaram diferenças significativas considerando a aplicação final desejada. A 4NC foi encapsulada sozinha, obtendo-se uma EE% maior que 99%. O perfil de liberação da 4NC também foi obtido para pH 7,4 e ocorreu por difusão. As MNPs foram encapsuladas em diferentes concentrações e, por meio

de TGA, observou-se que quanto maior a porcentagem inicial de MNPs, menor a EE%. Além disso, pode-se observar que usando um tetratiol na formulação, em vez de um ditiol, a EE% também é maior. Desta forma, os materiais sintetizados demonstraram potencial para serem aplicados na área biomédica e, mais especificamente, no tratamento do câncer.

Palavras chave: Polimerização tiol-eno. Nanopartículas magnéticas. 4-nitrochalcona. Miniemulsão. Nanoencapsulação.

RESUMO EXPANDIDO

Introdução

Nanopartículas poliméricas são sistemas carreadores de fármacos que apresentam diâmetro inferior a 1 μm, podendo variar de tamanho dependendo do campo de aplicação (SCHAFFAZICK et al., 2003). Existem vários métodos relatados na literatura para a preparação de nanopartículas poliméricas e encapsulação de compostos. No processo de polimerização em miniemulsão, pequenas gotas de 50 a 500 nm são formadas pela dispersão, através de um equipamento de alto cisalhamento, de um sistema contendo a fase dispersa e a fase contínua e, posteriormente, polimerizadas pela adição de iniciador e aumento da temperatura (LANDFESTER, 2006). Na técnica de polimerização via miniemulsificação e evaporação de solvente, o polímero pré-formado é dissolvido juntamente com os demais componentes e, em seguida, tal solução é dispersa na fase contínua, através de um equipamento de alto cisalhamento. Após o solvente é removido por evaporação (MUSYANOVYCH et al., 2008; PICH et al., 2006). Ambos os métodos possuem a vantagem de ser possível encapsular compostos inorgânicos. Contudo, através da polimerização em miniemulsão isto é possível em apenas uma etapa. A polimerização tiol-eno ocorre como uma polimerização tradicional por radicais livres com as etapas de iniciação, propagação e terminação, mais uma etapa de transferência de cadeia. No mecanismo fundamental de transferência de cadeia, um carbono central transfere seu elétron a um grupo tiol. Geralmente, utiliza-se uma proporção tiol:eno de 1:1, com o intuito de evitar reações secundárias. Reações de polimerização tiol-eno começaram a ser exploradas pelos pesquisadores somente a partir de 2014. Estas reações são bastante atrativas, inclusive para aplicações biomédicas, devido às suas características únicas, que incluem condições brandas e taxas rápidas de reação sem a formação de subprodutos (MACHADO; SAYER; ARAUJO, 2017). Nanopartículas magnéticas (NPMs) têm sido amplamente utilizadas em uma série de aplicações na área biomédica, como no transporte de fármaco direcionado à uma região específica do corpo, tratamento por hipertermia e ressonância magnética por imagem (SAHOO et al., 2013; XIE et al., 2015; ZHAO et al., 2014). Para estas aplicações, as NPMs devem ter, combinadas, propriedades de alta saturação magnética, propriedades superparamagnéticas e biocompatibilidade. As chalconas são compostos polifenólicos da família dos flavonoides associados à diversas atividades farmacológicas. São

encontradas em abundância em plantas comestíveis e são precursores metabólicos de outros flavonoides e isoflavonoides. Suas propriedades antioxidantes, efeitos citostáticos na tumorigênese e habilidade de inibir uma ampla variedade de enzimas, levou os pesquisadores a considerar estes compostos como anticarcinogênicos em potencial (SKIBOLA; SMITH, 2000). Com base no documento *World cancer report 2014* da *International Agency for Research on Cancer (Iarc)*, da Organização Mundial de Saúde (OMS), é inquestionável que o câncer é um problema de saúde pública. É uma das principais causas de morbidade e mortalidade no mundo, perdendo apenas para doenças cardiovasculares. Em 2015, foi responsável por 8,8 milhões de mortes, e estima-se que este número cresça cerca de 70% nas próximas duas décadas (FERLAY et al., 2015). No tratamento do câncer, a maior dificuldade é destruir as células tumorais sem afetar o tecido saudável no seu entorno. Nanopartículas poliméricas magnéticas têm sido consideradas um sistema eficaz, pois contribuem para a entrega precisa do fármaco no local desejado, reduzindo os efeitos colaterais e aumentando a eficácia terapêutica.

Objetivos
Este trabalho teve como principal objetivo a síntese e caracterização de nanopartículas superparamagnéticas de poli(tioéter-éster) (PTEe) com encapsulação do fármaco 4-nitrochalcona (4NC) como um agente anticâncer. Além disso foram obtidas a eficiência de encapsulação das MNPs e propriedades magnéticas das MNPs-PTEe obtidas via miniemulsificação e evaporação de solvente; viabilidade celular e internalização celular das MNPs-PTEe obtidas via miniemulsificação e evaporação de solvente; eficiência de encapsulação e perfil de liberação da 4NC encapsulada em nanopartículas de MNPs-PTEe obtidas via miniemulsificação e evaporação de solvente; e eficiência de encapsulação das MNPs e propriedades magnéticas das MNPs-PTEe obtidas via polimerização em miniemulsão.

Metodologia
PTEe foi sintetizado via polimerização tiol-eno em miniemulsão usando um monômero α,ω-dieno totalmente renovável obtido a partir do ácido 10-undecenóico e do 1,3-propanodiol, ambos derivados do óleo de mamona, conforme descrito por Cardoso et al. (2017). As MNPs foram sintetizadas por coprecipitação em meio aquoso, conforme descrito por Feuser et al. (2015). As MNPs e a 4NC foram encapsuladas primeiramente via miniemulsificação e evaporação de solvente utlizando

o polímero pré-pronto liofilizado. As MNPs e a 4NC foram encapsuladas também, separadamente, via polimerização em miniemulsão. Os métodos de caracterização utilizados foram TEM para caracterização morfológica; DLS para tamanhos de partícula, índice de polidispersão e potencial zeta; TGA para a eficiência de encapsulação das MNPs; FT-IR para caracterização química; VSM para determinar as propriedades magnéticas dos materiais; viabilidade celular e microscopia de fluorescência para análise de citotoxicidade e internalização celular, respectivamente; e espectroscopia UV-VIS para determinação da eficiência de encapsulação e perfil de liberação da 4NC.

Resultados e Discussão
Através do método de miniemulsificação e evaporação de solvente, as nanopartículas sintetizadas apresentaram morfologia esférica, diâmetros entre 120 e 150 nm e baixos índices de polidispersão. Análises de FT-IR mostraram tanto as bandas características do polímero quanto das NPMs. Análises de TGA mostraram uma eficiência de encapsulação das NPMs maior que 99%. Análises de VSM comprovaram que o material possui características superparamagnéticas. O ensaio de citotoxidade em células HeLa demonstrou que o material não é citotóxico. O ensaio de microscopia de fluorescência também em células HeLa demonstrou que, quando expostas à um campo magnético externo, a internalização das nanopartículas em células é até três vezes maior. A eficiência de encapsulação da 4NC foi superior a 90 %. O perfil de liberação da 4NC foi obtido para pH 7,4 e 6,0, utilizando amostra de NPMs e 4NC simultaneamente encapsuladas. Foi observado que a liberação ocorre por difusão e mais rapidamente em pH 6,0. Tal resultado era esperado, com base em estudos de liberação encontrados na literatura. Utilizando o método de polimerização em miniemulsão, as nanopartículas também apresentaram morfologia esférica, porém diâmetros e índices de polidispersão um pouco mais altos. O fármaco 4NC foi encapsulado separadamente, obtendo-se uma eficiência de encapsulação maior que 99 %. O perfil de liberação da 4NC deste foi obtido para pH 7,4, ocorrendo também por difusão. As NPMs foram encapsuladas em diferentes concentrações e observou-se que quanto maior a porcentagem inicial de NPMs, menor a eficiência de encapsulação das mesmas. Além disso, pode ser observado que utilizando um tetratiol na formulação, ao invés de um ditiol, a eficiência de encapsulação de NPMs foi maior.

Considerações Finais

Nanopartículas superparamagnéticas e o agente anticarcinogênico 4-nitrochalcona foram encapsulados com sucesso em nanopartículas de PTEe utilizando-se dois métodos diferentes. As nanopartículas apresentaram morfologia esférica, diâmetros dentro da faixa para a aplicação desejada e provaram ter comportamento superparamagnético. Análises TGA mostraram altas eficiências de encapsulação das MNPs para ambos os métodos. Contudo, observou-se que, para o método de polimerização em miniemulsão, quanto maior o percentual inicial de MNPs, menor o seu% de EE. Além disso, pode-se observar que usando um tetratiol na formulação, em vez de um ditiol, a% EE de MNPs foi maior. Este método apresenta a vantagem de poder incorporar MNPs em apenas uma etapa. Ensaios de citotoxicidade em células HeLa demonstraram que o material não é citotóxico. E o ensaio de microscopia de fluorescência, também em células HeLa, demonstrou que, quando exposta a um campo magnético externo, a captação celular é até três vezes maior. Embora mais ensaios sejam necessários para comprovar sua eficácia, os materiais sintetizados demonstraram potencial para serem utilizados em aplicações biomédicas, como o tratamento do câncer.

Palavras chave: Polimerização tiol-eno. Nanopartículas magnéticas. 4-nitrochalcona. Miniemulsão. Nanoencapsulação.

ABSTRACT

Cancer is one of the leading causes of morbidity and mortality in the world, thus it is nowadays considered as a public health problem. The greatest difficulty during the treatment is to destroy the tumor cells without affecting the healthy tissue. Magnetic polymeric nanoparticles have been considered as an effective system as they contribute to a precise drug delivery, reducing side effects and increasing the therapeutic efficacy. Chalcones are polyphenolic compounds of the flavonoid class associated with various pharmacological activities, whose properties led researchers to consider them as potential anticarcinogens. Thiol-ene polymerization is a new and promising field of study due to its attributes, including mild conditions and rapid reaction rates without the formation of byproducts. Herein, superparamagnetic poly(thioether-ester) nanoparticles along with the encapsulation of 4-nitrochalcone (4NC) were synthesized for the first time. Thiol-ene polymerization in miniemulsion was applied using a fully renewable α,ω-diene monomer obtained from 10-undecenoic acid and 1,3-propanediol, both derived from castor oil. Superparamagnetic nanoparticles were successfully synthesized by miniemulsification and solvent evaporation, presenting spherical morphology, diameters around 135 nm and low polydispersity indexes. FT-IR analyses showed the absorption bands of both the polymer and the MNPs. TGA analyses showed an encapsulation efficiency (EE%) of MNPs greater than 99%. Cytotoxicity and fluorescence microscopy assays in HeLa cells have demonstrated that the material is not cytotoxic and that, when exposed to an external magnetic field, the cell uptake is up to three times higher. The EE% of 4NC was greater than 90%. The release profile of 4NC was obtained at pH 7.4 and 6.0, using a sample of MNPs and 4NC simultaneously encapsulated. It was observed that the release occurs by diffusion and faster at pH 6.0. Nanoparticles were also synthesized by mininemulsion polymerization, which has the advantage of incorporating inorganic compounds in only one step. Characteristics such as morphology, diameter and polydispersity index did not present significant differences considering the desired final application. The 4NC was encapsulated alone, obtaining an EE% greater than 99%. The 4NC release profile was also obtained for pH 7.4 and it occurred by diffusion. The MNPs were encapsulated at different concentrations and, through TGA, it was observed that the higher the initial percentage of MNPs, the lower the EE%. In addition, it could be seen that using a tetrathiol in the formulation, rather than a dithiol, the EE% of MNPs was greater. In this

way, the synthesized materials demonstrated potential to be applied in the biomedical area and, more specifically, in the treatment of cancer.

LIST OF FIGURES

LIST OF TABLES

ABREVIATIONS LIST

4NC	4-nitrochalcone
AIBN	Azobisisobutyronitrile
BDT	1,4-buthanedithiol
DCM	Dichloromethane
DLS	Dynamic Light Scattering
DMSO	Dimethyl sufoxide
DOX	Doxorrubicin
Dp	Particle size
EE%	Encapsulation efficiency
FT-IR	Fourier Transform Infrared Spectroscopy
H	Magnetic field
H_c	Coercive field
HPT	Hyperthermia
IARC	International Agency for Research on Cancer
INCA	Instituto Nacional do Câncer
KPS	Potassium persulfate
M	Magnetization
MEM	Minimum essential medium
MNPs	Magnetic nanoparticles
M_r	Remaining magnetization
MRI	Magnetic resonance imaging
M_s	Saturation magnetization
NPs	Nanoparticles
OA	Oleic acid
PBS	Phosphate buffer saline
PdI	Polydispersity index
PDT	Photodynamic therapy
PETMP	Pentaerythritol tetrakis(3-mercaptopropionate)
PTEe	Poly(thioether-ester)
SDS	Sodium dodecyl sulfate
SPMNPs	Superparamagnetic nanoparticles
TEM	Transmission Electron Microscopy
TGA	Themogravimetric analysis
VSM	Vibrating Sample Magnetometer
WHO	World Health Organization

CHAPTER I

1 INTRODUCTION

Currently, it is undeniable that cancer is a public health problem. It is one of the main causes of morbidity and mortality in the world, second only to cardiovascular disease. In 2015, it was responsible for 8.8 million deaths, and this number is expected to grow about 70% over the next two decades (STEWART; WILD, 2014). Among developing countries, the impact of cancer in the population is even higher. It is expected to account for 80 % of the more than 20 million new cases estimated in the coming decades (INCA, 2017). The greatest difficulty during cancer treatments is to destroy the tumor cells without affecting the healthy tissue in their surroundings, which happens in conventional therapies such as chemotherapy and radiotherapy. Hence, there is a great effort to develop more selective methods for the treatment of this disease.

Magnetic nanoparticles (MNPs) have important biomedical applications as theranostic systems as they allow for the concomitant magnetically targeted drug delivery and tissue imaging through magnetic resonance imaging (MRI) (SOARES et al., 2016; XIE et al., 2015). Furthermore, magnetic nanoparticles can kill targeted cells (e.g., tumor cells) by hyperthermia, i.e., the development of lethal heat by applying external alternating magnetic field at the tumor site (FEUSER et al., 2015a; PATIL et al., 2014). The physical properties such as size, shape, hydrophilic nature, surface charge, and magnetic behaviour are responsible for their biodistribution and biocompatibility. The chemical properties such as composition of the core and coating are also responsible for biocompatibility, as well as for binding different molecules for therapeutic efficacy (GUPTA; GUPTA, 2005). The dual-functional nature of MNPs as both imaging agent and a carrier for target specific pharmaceutics under a magnetic field gradient has made them attractive delivery agents *in vitro* and *in vivo*.

Chalcones are part of a select group of chemical compounds associated with various pharmacological activities. They are not only important precursors for synthetic manipulations, but also form a major component of natural products. Its antioxidant properties, cytostatic effects on tumorigenesis and the ability to inhibit a wide variety of enzymes, led the researchers to consider chalcones as potential anticarcinogens (SKIBOLA; SMITH, 2000). In addition, chalcones have other known biological activities, such as: hypocholesterolemic,

antinociceptive, immunomodulatory, anti-inflammatory, antibacterial, antifungal and antiviral (BHAT et al., 2005; NOWAKOWSKA, 2007). The 4-nitrochalcone, which is the compound applied in this study, some studies have been published showing its action on several cell lines (DALLA VIA et al., 2009; DIMMOCK et al., 2002; ILANGO; VALENTINA; SALUJA, 2010). Some results suggest that 4-nitrochalcone has a selective effect on tumor cells, which is important to reduce toxic effects on health cell during cancer treatment (ESCOBAR, 2014).

The use of polymeric nanoparticles for drug delivery results in higher and localized concentrations of the drug in a specific site, reducing the toxic effects on healthy cells or tissues, providing a strategy for the diagnosis and treatment of diseases. Polymeric nanoparticles can be prepared from natural or synthetic polymers (LANDFESTER; MAILÄNDER, 2013). Natural and synthetic biodegradable polymers have prospective applications in drug delivery because they can be breakdown into smaller molecules under specific biological stimuli (MACHADO; SAYER; ARAUJO, 2017).

The thiol-ene polymerization is a promising tool for synthesizing polymeric nanoparticles (JASINSKI et al., 2014, 2016) with potential for biomedical applications. Innovative biomaterials are arising from this technique due to the interest on its unique attributes, including mild reaction conditions, fast reaction rates, and without formation of by-products (JASINSKI et al., 2014). The thiol-ene polymerization in miniemulsion is a new field of study. Only after 2014, articles describing the synthesis of linear polymers by thiol-ene polymerization have been published (AMATO et al., 2015; CARDOSO et al., 2017; JASINSKI et al., 2014). Besides avoiding the use of organic solvents, the major advantage of miniemulsion polymerization is the possibility of producing complex nanostructures, including the encapsulation of inorganic nanoparticles, in a single reaction stage and with high polymerization rates (LANDFESTER; MAILÄNDER, 2013; MAHDAVIAN; ASHJARI; MOBARAKEH, 2008; QIU et al., 2007).

Another method of polymerization is the miniemulsification and solvent evaporation method, in which a preformed polymer is used in the first step to be dissolved together with the other components, such as the drug previously solubilized in the solvent. In this reaction, less surfactant is needed, when compared to the emulsification and solvent evaporation technique (LEIMANN et al., 2013). Moreover, this is an interesting method from an economic point of view, since water is used as a non-

solvent. It simplifies and reduces the costs of the process, besides eliminating the need for recycle and facilitating the washing step to remove any impurities (PINTO REIS et al., 2006).

A large number of studies have been developed regarding the encapsulation of MNPs in polymeric colloidal particles, applying several methods of polymerization (M. VAN HERK; LANDFESTER, 2010; ROMIO et al., 2013; STAUDT et al., 2013). Some studies have also shown a significant improvement in cellular uptake of MNPs into tumor cells when an external magnetic field was applied (ANGELOPOULOU et al., 2017; PRIJIC et al., 2010). And the simultaneous encapsulation of drugs and MNPs has been studied as well (FEUSER et al., 2015b; THORAT et al., 2016, 2017). Nevertheless, thiol-ene polymerization in miniemulsion, as well as nanoencapsulation of 4NC specifically for the treatment of cancer, has not yet been explored in the literature.

The miniemulsion polymerization research group of the Laboratory of Process Control (LCP) from the Federal University of Santa Catarina has been working with thiol-ene miniemulsion polymerization since 2015, aiming at the use of monomers obtained from renewable sources (CARDOSO et al., 2017; MACHADO et al., 2017; MACHADO; SAYER; ARAUJO, 2017). The encapsulation of MNPs and drugs has also been explored by the group, seeking to apply these biobased materials and others, which synthesis is already known, in the biomedical area (CARDOSO et al., 2017; CHIARADIA et al., 2015, 2016, FEUSER et al., 2015a, 2015b, 2016). This work places itself in this context, using MNPs and an anticancer drug very little studied, incorporated in an environmentally friendly polymeric matrix.

1.1 OBJECTIVES

1.1.1 General objective

The main goal of this work was the synthesis, characterization and *in vitro* assays of magnetic nanoparticles and 4-nitrochalcone simultaneously encapsulated in poly(thioether-ester) nanoparticles obtained by minemulsification and solvent evaporation, as well as the miniemulsion polymerization method.

1.1.2   Specific objectives

- Encapsulation efficiency of MNPs and magnetic properties of MNPs-PTEe nanoparticles obtained via miniemulsification and solvent evaporation;
- Cell viability assay and cellular uptake of MNPs-PTEe nanoparticles obtained via miniemulsification and solvent evaporation;
- Encapsulation efficiency and release profiles of 4NC loaded in MNPs-PTEe nanoparticles obtained by miniemulsification and solvent evaporation;
- Encapsulation efficiency of MNPs and magnetic properties of MNPs-PTEe nanoparticles obtained by miniemulsion polymerization.

CHAPTER II

This chapter presents a literature review about the main subjects discussed in this dissertation, including the nanoparticles obtention methods used in this research, magnetic nanoparticles and chalcones as anticancer agents.

2   LITERATURE REVIEW

2.1 POLYMERIC NANOPARTICLES

Nanosized particles have attractive characteristics, which have received considerable attention in the last decade. Polymeric nanoparticles (NPs) are solid particles or particulate dispersions with size in the range of 10–1000 nm, varying in size depending on the field of application (MALLAKPOUR; BEHRANVAND, 2016; SCHAFFAZICK et al., 2003). These nanoparticles can be also classified as nanospheres or nanocapsules. In the nanospheres, the encapsulated compound is homogeneously dispersed or solubilized in the polymer matrix, obtaining a monolithic system in which it is not possible to identify a differentiated nucleus. The nanocapsules are vesicular systems in which the encapsulated material is confined in a cavity, consisting of a core-liquid interior surrounded by a polymeric matrix (PINTO REIS et al., 2006).

There are several methods reported in the literature for the preparation of polymer nanoparticles, which can generally be classified in methods based on the *in situ* polymerization of dispersed monomers or on the precipitation of preformed polymers (SCHAFFAZICK et al., 2003). Among the main methods for the preparation of NPs *in situ*, it is possible to highlight the polymerization in miniemulsion. For the technique of polymerization with preformed polymers, the miniemulsification and solvent evaporation method stands out.

2.2 RENEWABLE MONOMERS

In a time of rising oil prices, global warming and other environmental problems, the use of renewable raw materials can make a significant contribution to sustainable development. Currently, vegetable oils are the most important renewable raw material for the chemical industry. They are triglycerides with different fatty acid compositions, depending on the plant, crop, season, and plant growth conditions. Fatty

acids constitute 95% of the total weight of the triglycerides and their content is characteristic for each vegetable oil (MONTERO DE ESPINOSA; MEIER, 2011).

Fatty acids have long been used by scientists for the development of polymeric structures, either directly or as building blocks for the synthesis of more sophisticated monomers. Fatty acids are valuable renewable building blocks for the synthesis of monomers that contain specific properties and do not require extensive chemical modification prior to their application (MONTERO DE ESPINOSA; MEIER, 2011). Recently, the application of triglycerides in polymer science has been evaluated by focusing on crosslinked systems for applications such as coatings and resins, with the conclusion that triglycerides have the potential to play a key role during the 21st century in the synthesis of polymers from renewable sources (MEIER; METZGER; SCHUBERT, 2007).

2.3 ENCAPSULATION

Encapsulation is defined as the "packaging" technology of active materials in the form of solids, liquids or even gaseous. These materials are encapsulated in polymer layers that can release the material under specific conditions and at controlled rates of speed and quantity (GIBBS et al., 1999). It was originally introduced in the field of biotechnology to make production processes more efficient as the matrix around the cells allows the rapid and efficient separation of producer cells and their metabolites. These technologies, developed around 60 years ago, are of significant interest to the pharmaceutical industry, in particular for the release of drugs and vaccines (NEDOVIC et al., 2011).

Gibbs et al. (1999) referred to the encapsulated material as the active agent or core and the material covering the core as a membrane, a carrier, or, as more commonly referred to as a wall. The particles obtained by the encapsulation processes can be classified by size into three categories: macro- (> 5000 μm), micro- (0.2-5000 μm) and nanocapsules (<0.2 μm). In terms of architecture, they can be divided into two groups: those in which the nucleus is clearly concentrated in the central region, surrounded by a defined and continuous film of the wall material, and those in which the nucleus is evenly dispersed in a matrix (BAKER, 1986), as shown in Figure 1.

Figure 1. Microsphere (A); single microcapsule (B); simple, irregular (C); two walls (D); several nuclei (E); clustering of microcapsules (F).
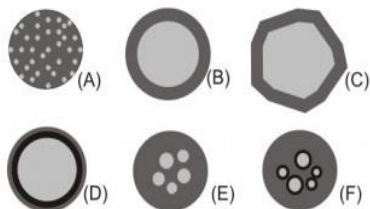
Source: Adapted from ARSHADY, 1993.

The choice of the encapsulation method for a specific application depends on a number of factors, such as required particle size, physical and chemical properties of the core and wall, application of the final product, desired release mechanisms, production scale and cost (RÉ, 1998). Several encapsulation methods are found in the literature. Among them, the miniemulsion polymerization can be mentioned, in which particles are formed by the dispersion of a system containing the monomer and co-stabilizer in water and surfactant and are then polymerized (LANDFESTER, 2006); the emulsification and solvent evaporation method, which involves the preparation of an emulsion consisting of the dissolution of a preformed polymer in a water immiscible organic solvent and the aqueous phase. The organic solvent is evaporated under increasing temperature causing formation of stable nanoparticles in the aqueous phase (MUSYANOVYCH et al., 2008); and the miniemulsification and solvent evaporation method, which occurs when the emulsification of the organic and aqueous phase occurs in the presence of a high efficiency dispersing apparatus, such as an ultrasound probe, resulting in submicron particles, which differs it from the previous method.

2.3.1 Miniemulsification and solvent evaporation polymerization

The polymerization technique via miniemulsification and solvent evaporation is divided into three steps. First, the preformed polymer is dissolved together with the other components, such as the drug previously solubilized in the solvent. Then, such solution is dispersed in water containing surfactant forming stable nanometric droplets. In this step, a high efficiency energy source is required, such as ultrasonic generating sources, high pressure homogenizers or high efficiency mechanical

dispersers. In the latter step, the solvent is removed by extraction or evaporation. With the decrease of the amount of solvent in the droplets during their removal, the nanoparticles are formed as a function of the decrease of the solubility of the polymer in the solvent and its consequent precipitation (MUSYANOVYCH et al., 2008; PICH et al., 2006). In addition, less surfactant is needed, when compared to the emulsification and solvent evaporation technique, in order to avoid the formation of micelles and the polymer/organic solvent ratio is higher, i.e., less organic solvent is required for the dissolution of the polymer, since the initial droplet size has submicron proportions (LEIMANN et al., 2013).

The size of the nanoparticles can be controlled by adjusting the agitation rate, type and amount of dispersing agent, organic and aqueous phase viscosity, polymer concentration in the organic solvent, and temperature. The control of the characteristics of particle size distribution, mean diameter and morphology is important in the preparation stages, as they strongly interfere with performance during final application (POLETTO et al., 2008).

However, this technique only applies to lipophilic drugs and has limitations in scaling because of the large amount of energy required for homogenization (TRIERWEILER; TRIWERWEILER, 2011). On the other hand, although different types of emulsions can be used, this method is interesting from an economic point of view, since water is used as a non-solvent. It simplifies and reduces the costs of the process, besides eliminating the need for recycle and facilitating the washing step to remove any impurities (PINTO REIS et al., 2006).

2.3.2   Miniemulsion polymerization

In general, miniemulsions consist of submicron-sized and stable droplets distributed in a continuous phase. The high stability of the particles is ensured by the combination of the surfactant, which stabilizes the particles electrostatically or sterically, and the co-stabilizer, which is soluble and homogeneously distributed in the dispersed phase and prevents diffusional degradation by introducing a counter force to the Laplace pressure (ASUA, 2014; HIGUCHI; MISRA, 1962; LANDFESTER, 2009). The miniemulsion polymerization allows the synthesis of polymer nanoparticles with unique characteristics, of great commercial interest, since it is possible to incorporate water-insoluble compounds (ASUA, 2014; CRESPY; LANDFESTER, 2010; HIGUCHI; MISRA, 1962; LANDFESTER, 2009).

The miniemulsion polymerization technique differs from conventional emulsion polymerization. In the emulsion polymerization, the monomer leaves the droplets, forming the oligomer in the aqueous phase by reaction with radicals from the decomposition of a hydrophilic initiator and, when it becomes hydrophobic by increasing the non-polar chain, enters the micelles, as shown in Figure 2. In the miniemulsion polymerization process, the first stage consists of the formation of small drops of 50 to 500 nm by the dispersion of a system containing the dispersed phase (monomer and co-stabilizer) and the continuous phase (water and surfactant). The system is obtained through a high shear apparatus, for example an ultrasound probe. In the second step, these droplets are polymerized by addition of initiator – which may be hydrophilic or hydrophobic – and increase in temperature. The size of the droplets, directly after the preparation of the miniemulsion, depends mainly on the quantities and types of surfactant, co-stabilizer and the dispersion conditions (LANDFESTER, 2006).

Figure 2. Miniemulsion polymerization scheme.
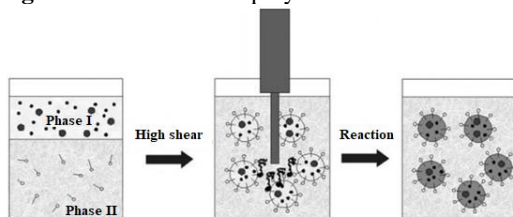
Source: Adapted from LANDFESTER (2009).

The major advantage of this technique is the possibility of producing complex nanostructures, including the encapsulation of inorganic nanoparticles, in a single reaction stage and with high polymerization rates (LANDFESTER; MAILÄNDER, 2013; MAHDAVIAN; ASHJARI; MOBARAKEH, 2008; QIU et al., 2007). Further, the miniemulsion polymerization technique has advantages such as better control of particle size by directly dispersing the hydrophobic inorganic particles in the monomer-containing phase with the aid of a stabilizer, nucleate all droplets containing inorganic particles and, depending on the formulation, produce dispersions of biocompatible nanoparticles (LANDFESTER; MAILÄNDER, 2013; QIU et al., 2007). On the other hand, a problem of this method is that the co-stabilizer

remains in the polymer nanoparticles after polymerization and may have a negative effect on the properties of the polymer (ASUA, 2002).

2.3.3   Thiol-ene polymerization

Thiol-ene polymerization occurs as a traditional free radical polymerization with the initiation, propagation and termination steps, plus a chain transfer step. In the fundamental mechanism of chain transfer, a central carbon transfers its electron to a thiol group. Generally, a thiol:ene ratio of 1:1 is used, in order to avoid side reactions, for example, where disulfide is formed. It is important to note that suitable copolymerization between the olefin and thiol molecules will only occur if the former is a diene and the latter a dithiol (MACHADO; SAYER; ARAUJO, 2017).

The reaction mechanism involves three steps (Figure 3). First, a thiol is decomposed into thiyl radicals by the elimination of a hydrogen, which may be by photo or thermo initiation, with or without the aid of initiators. Then, the thiyl radical is incorporated into the alkene by attacking its double bond. Finally, the chain transfer occurs because the unpaired electron generated in the central carbon of the formed chain is transferred to another thiol group and another thiyl radical is generated, restarting the cycle. Thus, thiol-ene polymerization revolves around the alternation between the propagation of thiyl radicals between the functional groups ene and chain transfer reactions (MACHADO; SAYER; ARAUJO, 2017).

Figure 3. Thiol-ene polymerization reaction scheme.
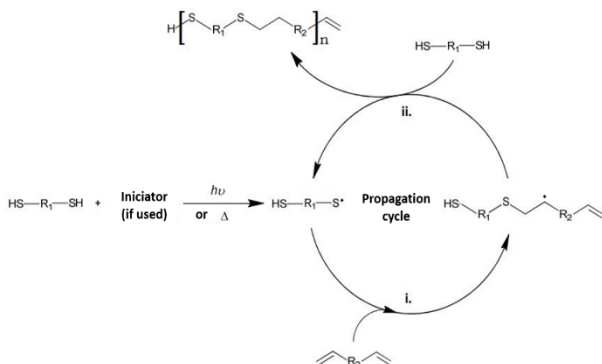
Source: Adapted from MACHADO; SAYER; ARAUJO (2017).

Cramer and Bowman (2001) used real-time Fourier Transform Infrared to monitor the conversion of the thiol and ene functional groups, independently, during photo-induced thiol-ene polymerization. From these results, the stoichiometry of thiol-ene and thiol-acrylate polymerizations were determined. In this study, it has been demonstrated that thiol-ene systems can be initiated with different types of initiators, including photopolymerization without the aid of a photoinitiator.

Yoshimura et al. (2015) used eugenol as a starting material for thiol-ene photopolymerization for the production of resins. Biologically based polymers were successfully synthesized by thiol-ene photopolymerization via allyl-etherified eugenol derivatives. Its thermal and tensile properties varied according to the functionality of the allyl and thiol groups, the conversion of the thiol-ene reaction, and the difference of the central structures in the polythiol compounds.

2.4 MAGNETIC NANOPARTICLES (MNPs)

Iron oxides have been the subject of studies at the nano scale more than any other material for decades. These oxides exist in many forms in nature, such as magnetite (Fe_3O_4), maghemite (Fe_2O_3) and hematite (α-Fe_2O_3), the latter being probably the most common (TEJA; KOH, 2009). The first work on this subject was published by Stoner and Wolhfarth (1948) and until the 1960s many nanometric scale iron oxide preparation techniques had already been developed, with the speculation that these oxides could have applications also in the biological and medical field (GRADY, 2002). From these studies, many others have been developed and various methods of preparing iron oxides have been described. For a given application, whether technological or biomedical, the preparation methods can influence the final characteristics of the material, thus, each preparation method must be specific for a given application (GRADY, 2002).

2.4.1 Applications

The magnetic properties of iron oxides have been exploited in a wide range of applications, including magnetic seals, inks, magnetic engraving, catalysts and ferrofluids. For biomedical applications, MNPs fall into two categories: those involving *in vivo* use and *in vitro* use.

As an example of *in vivo* application, magnetic resonance imaging (MRI) can be mentioned, which has well-known applications in

the diagnostic area as a contrast (ZHANG et al., 2004); drug release because, in addition to their reduced size and low toxicity, MNPs can be transported by a magnetic field, penetrating deeply into human tissue (GUPTA; WELLS, 2004); and hyperthermia, which is utilized to "burn" cancer cells, often in combination with chemotherapy (LANDFESTER; RAM REZ, 2003), it being known that cancer cells are more sensitive to temperatures higher than 41 °C than their normal counterparts.

As an example of *in vitro* applications, cell isolation can be cited, in which the exposure of MNPs to an external magnetic field allows the separation of a wide variety of biological entities. Thus, it is possible, for example, the isolation of cancer cells in blood samples, which can provide a better diagnosis of the disease (GRADY, 2002). In spite of this wide range of applications in the biomedical area, some of these applications may present risks, being of fundamental importance the understanding of its properties and interactions with cells, tissues and organs of the human body, which is considered a scientific challenge that must be approached to verify the feasibility of using nanobiotechnology in biomedical applications (LANDFESTER; RAM REZ, 2003).

A number of strategies have been proposed in the literature to encapsulate MNPs in colloidal polymer particles, including emulsion polymerization (M. VAN HERK; LANDFESTER, 2010), reverse miniemulsion polymerization (ROMIO et al., 2013) and direct miniemulsion polymerization (HE et al., 2009; LANDFESTER; RAM REZ, 2003; STAUDT et al., 2013). However, it is important that the MNPs have, combined, properties of high magnetic saturation, superparamagnetic properties and biocompatibility in order to be applied in the biomedical field.

2.4.2   Magnetic properties

According to Rezende (1996), depending on the microscopic origin of its magnetization and internal interactions, materials are commonly classified into five categories: diamagnetism, paramagnetism, ferromagnetism, ferrimagnetism and antiferromagnetism. When we talk about the magnetic properties of iron oxides, depending on temperature and volume, they can have paramagnetic, ferromagnetic, ferrimagnetic and superparamagnetic properties. The magnetite presents ferromagnetic properties in the micrometric scale and superparamagnetic properties in the nanometric scale (10-20 nm) (DAVE; GAO, 2009).

Ferromagnetic materials when demagnetised are divided into small regions, named domains, where all magnetic moments are ordained. When a sample is placed in an external magnetic field the domains tend to align with the field (Figure 4) reaching a maximum magnetization value (degree of saturation) (SINNECKER, 2000). When the material has a very small size, the domains merge into a single one, generating a mono-domain particle. The size for which a nanostructured material changes from multi-domain to mono-domain depends on each material, and it is known as critical size or critical diameter, if the particle formed is spherical. When the particles have diameter greater than the critical diameter, this material presents as multi-domain; if the diameter is smaller than the critical one, it presents mono-domain.

Figure 4. Magnetic behavior of ferromagnetic and superparamagnetic nanoparticles when exposed to an external magnetic field.
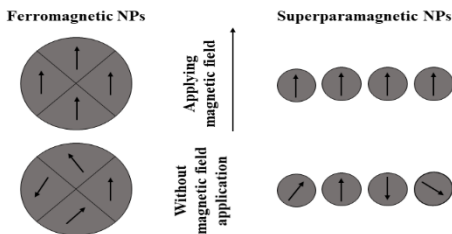
Source: Adapted from DAVE; GAO, 2009.

In Figure 5 it is possible to observe the characteristic behaviour of the magnetization (M) of a material magnetically hard like tempered steel (prepared by heating, followed by abrupt cooling) as a function of the magnetic field (H). Applying a magnetic field in the material initially demagnetized, it will follow a curve until reaching a constant plateau called saturation magnetization (M_s). By decreasing the magnetic field from this value, M_s decreases more slowly following the direction given by the arrow, until a residual value of the magnetization for a null magnetic field called the remaining magnetization (M_r). The material remains magnetized without magnetic field application, such as refrigerator magnets. By reversing the direction of the field and following in the same direction of the curve, for values of M smaller than Mr until the magnetization cancels out for a certain magnetic field value, we reach the point called the coercive field (H_c) (SINNECKER, 2000). In this case, if we continue to vary the magnetic field module, we come back to a

region of saturation and repeating the cycle in the opposite direction a closed curve is obtained, which is called a hysteresis cycle.

Figure 5. Hysteresis curve.
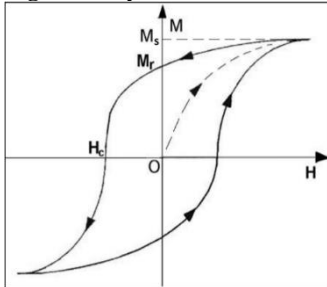
Source: RIBEIRO, 2000.

Materials with extremely small dimensions, such as magnetite nanoparticles, present a magnetic mono-domain. In this context, each atom of a particle is part of an arrangement magnetically aligned in a single direction and therefore the total magnetic moment is the sum of all the atomic moments of the particle (CULLITY, 1972). When a mono-domain particle is uniformly magnetized with spins pointed in a single direction, the magnetization will be reversed by spins rotations, since there is no wall to prevent it. Thus, as the Hc required to reduce the magnetization to zero will be high, the mono-domain nanoparticles will exhibit high Hc. This effect begins when the particles begin to decrease and the thermal energy begins to equate with the energy required to reverse the spin direction, forming a superparamagnetic state. A particle is said to be superparamagnetic at a given temperature if its characteristic time, or relaxation time, is less than the time required to perform the measurement. Figure 6 shows a curve of a material that does not manifest hysteresis in the magnetization process, typical of a superparamagnetic material (KNOBEL, 2000).

Figure 6.Superparamagnetic material's curve.
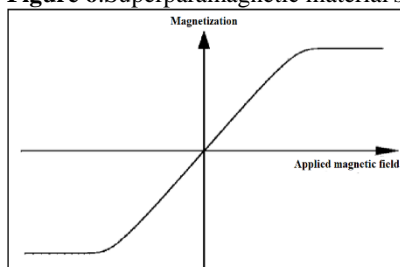
Source: Adapted from SINNECKER, 2000.

2.4.3   Preparation methods

The advancement in the use of MNPs for biomedical applications depends on a synthesis method in which there is a control of the nanoparticle size distribution, its magnetic properties and surface characteristics (GUPTA; WELLS, 2004). Magnetite nanoparticles can be prepared by a variety of physical and chemical methods. Among the physical methods, the method of colloidal sols by disaggregation, by vapor deposition and carbon arc deposition can be highlighted (DURÁN et al., 2006). Among the chemical procedures, the methods of co-precipitation in microemulsion (reverse micelle), decomposition of compounds by coordination, sonification decomposition, reduction of metallic ions and co-precipitation in aqueous medium can be highlighted (TARTAJ et al., 2003).

However, the co-precipitation method in aqueous media is the most used, due to its possibility to easily regulate the pH value and size of the nanoparticles, factors that are of extreme importance for the final quality of the MNPs (ZHU; WU, 1999). The preparation of the MNPs by this method consists in the co-precipitation of the metallic ions in aqueous solutions through reactions of alkaline hydrolysis (DURÁN et al., 2006). From this method it is possible to produce magnetite nanoparticles with the addition of oleic acid, which allows its suspension and stabilization (ZHANG et al., 2004).

2.5 CHALCONES

Throughout the ages, mankind has always been dependent on nature, especially on plants, as a source of carbohydrates, proteins and fats for nourishment or as a means of sheltering. Additionally, plants are

a valuable source of a wide range of secondary metabolites, which are used as pharmaceutical compounds, agrochemicals, flavorings, fragrances, colorants, biopesticides and food additives. Thus, plants formed the basis of traditional medicine (RAMACHANDRA RAO; RAVISHANKAR, 2002).

Natural products have shown promising anticancer activity. They were the mainstay for the use of chemotherapy against cancer, and the flavonoids remained as the main compound used (MAHAPATRA; BHARTI; ASATI, 2015). Flavonoids are a group of heterogeneous, heat-resistant polyphenols that have beneficial health properties. They are found in fruits, vegetables, teas, wines and are generally subdivided into nine classes, including flavonols, flavones, flavonones, flavan-3-ols, anthocyanins, isoflavones, proanthocyanins, aurones and chalcones (SHAHIDI; AMBIGAIPALAN, 2015). Epidemiological studies suggest that flavonoid intake may reduce the risk of tumors in the breast, colon, lung, prostate, and pancreas (PRAKASH et al., 2013).

The basic structure of a flavonoid is the flavan nucleus, consisting of fifteen carbon atoms arranged in three rings (C_6-C_3-C_6), called A, B and C in Figure 7. The various classes of flavonoids differ in the level of oxidation and in the substitution pattern of the ring C, while individual compounds within a class differ in the substitution pattern of rings A and B (COWAN, 1999).

Figure 7. Basic structure of flavan (1) and chalcone (2).

Source: From the author.

Chalcones are polyphenolic compounds of the flavonoid family associated with various pharmacological activities. They are found in abundance in edible plants and are metabolic precursors of other flavonoids and isoflavonoids. Its antioxidant properties, cytostatic effects on tumorigenesis and the ability to inhibit a wide variety of enzymes led researchers to consider these compounds as potential anticarcinogens (SKIBOLA; SMITH, 2000). The privileged structure of chalcones remained a fascination among researchers in the 21st century because of their simple chemistry, ease of synthesis, diversity of substituents and

wide range of biological activities, as reported by Mahapatra et al. (2015). Chalcones and their derivatives can be synthesized by condensation of Claisen-Schimidt between a benzaldehyde in an acetophenone using a solution of sodium hydroxide as a catalyst (DETSI et al., 2009). Another method has also been reported in which irradiation with household microwave apparatus are used to synthesize these compounds (SRIVASTAVA, 2008).

2.5.1   Biological activities

A number of naturally occurring chalcones, as well as their derivatives, have been isolated from various sources and identified with different biological activities such as anti-inflammatory, antioxidant, antimicrobial and anticancer. The latter will be further explored below.

2.5.1.1   Anticancer activity

Among the anticancer agents already identified nowadays, chalcones represent an important class of molecules. Apoptosis dysregulation or programmed cell death in multicellular organisms are the factors that most contribute to the survival of tumor cells. The apoptosis process can be divided into two parts: sensors and effectors. The sensors (extrinsic path) are responsible for monitoring the conditions of the extra and intracellular environments, which define when a cell should live or die. These signals regulate the second class of components (intrinsic pathway or mitochondrial apoptosis), whose function is to induce cell death by apoptosis. The chalcones act both through the extrinsic and intrinsic pathways, preventing the tumor evolution (LIU et al., 1996).

Different geographical regions of the world at different time periods have documented the extensive use of licorice (*Glycerhiza glabra*) for curing different diseases in humans, for example as an anti-ulcer agent (FIORE et al., 2005). More modern studies have identified different chalcones and flavonoids as being the active compound responsible for such activities. Chalcones such as isoliquiretigenine, licochalcone A and licochalcone E, were isolated from licorice and reported to be efficient against a number of cancer cell lines (TAKAHASHI et al., 2004; XIAO et al., 2011; YOON; JUNG; CHEON, 2005). Xiaolin and Simoneau (2005) isolated flavokawain A from the Kava extract (*Piper mesthisticum*), finding that this compound is

suppressor of the growth of bladder tumors. In addition to the natural chalcones mentioned above, a number of chalcones have been synthesized and shown anticancer activity.

Hsu et al. (2006) analyzed the activity of chalcone in heart tumor cells (MCF-7 and MDA-MB-231) and observed the apoptosis induction by intrinsic route, due to the increased expression of Bax and Bak and subsequent activation of caspase-9. They also observed cell cycle arrest in G2/M by increasing the expression of p21 and p27 and reducing levels of cyclins after treatment, both at the dose of 10 μmol/L. Navarini et al. (2009) found that chalcones hydroxylated at positions 5 or 6 of the A-ring at the dose of 100 μmol/L had a greater cytotoxic effect on B16-F10 melanoma cells than methoxylated and hydroxylated chalcones in other positions. The authors attributed this effect to the induction of cell death by apoptosis, demonstrated by increasing DNA fragmentation.

Regarding nitrated chalcones, few biological effects have been described. The 4-nitrochalcone (Figure 8), the anticancer drug used in this work, has already had its antitumor activity described by some authors. Dimmock et al. (2002) found that after the 24-hour treatment with 4-nitrochalcone the L1210 leukemic cells the IC50 was 59 μmol/L, whereas for T-lymphocytes the IC50 was 13.8 μmol/L. Dalla Via et al. (2009) found that 4-nitrochalcone reduced the viability of JR8 melanoma cells and that the IC50 value of 6 μmol/L was obtained after 72 h of treatment. Ilango et al. (2010) observed that 4-nitrochalcone with treatment for 24 h decreases the viability of MCF-7 and T47D heart tumor cells having IC50 of 55 and 52 μmol/L, respectively. In the laboratory of biological oxidation and cell culture of the Federal University of Paraná, it was found that 4-nitrochalcone reduces approximately 50% of the viability of HEPG2 cells at a dose of 20 μmol/L at 24 h, whereas in L929 flibroblasts cells there was no change in viability at the same dose and treatment time. This result suggests a selective effect on tumor cells, which is important to reduce side effects in the treatment of cancer (ESCOBAR, 2014). Table 1 summarizes the studies mentioned above.

Figure 8. Structure of 4-nitrochalcone.
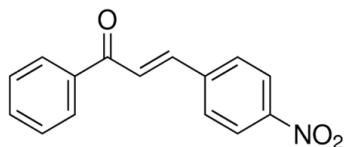
Source: From the author.

Table 1. Main studies regarding the use of 4NC as an anticancer agent.

Reference	Cell line	Treatment time (h)	IC50 (µmol/L)
DIMMOCK et al. (2002)	L1210 leukemic cells	24	59
	T-lymphocytes		14
DALLA VIA et al. (2009)	JR8 melanoma cells	72	6
ILLANGO et al. (2010)	MCF-7 heart tumor cells	24	55
	T47D heart tumor cells		52
ESCOBAR (2014)	HEPG2 cells	24	20
	L929 flibroblasts		-

Source: From the author.

2.6 CANCER

According to the brazilian National Cancer Institute (INCA), cancer is the name given to a set of more than 100 diseases that have in common the disordered growth of cells, which invade tissues and organs. Such cells tend to be extremely aggressive, as they divide rapidly and uncontrollably, and can form malignant tumors, which can spread to other regions of the body (INCA, 2018). It can be caused by external factors such as abusive and/or continuous use of toxic substances and an unhealthy diet, or internal factors such as hereditary genetic mutations, hormonal issues, and immune system conditions. Such factors may act together or in sequence to cause cancer (AMERICAN CANCER SOCIETY, 2015).

Based on the World Cancer Report 2014 document of the International Agency for Research on Cancer (IARC) of the World Health Organization (WHO), it is unquestionable that cancer is a public health problem. It is one of the leading causes of morbidity and mortality in the world, second only to cardiovascular disease, with approximately 14.1 million new cases (excluding non-melanoma skin cancers) and 8.2 million disease-related deaths in 2012 (STEWART; WILD, 2014). According to data from the GLOBOCAN/IARC project of 2012, the most common cancers in the world were lung (1.8 million), breast (1.7 million), intestine (1.4 million) and prostate (1 million). In 2015, it was responsible for 8.8 million deaths, and is expected to grow by about 70 % over the next two decades (FERLAY et al., 2015).

Among developing countries, the impact of cancer in the population is expected to account for 80 % of the more than 20 million new cases estimated in the coming decades. In Brazil, the estimate for the

biennium 2018-2019 indicates the occurrence of about 600 thousand new cases of cancer, and, except for cases of non-melanoma skin cancer, the most frequent would be prostate cancer in men (31.7 %) and breast cancer in women (29.5 %) (INCA, 2017).

2.6.1 Cancer treatment

Cancer treatments include surgical interventions, chemotherapy, radiotherapy, hormone therapies, immune therapy and targeted therapies, in which the drug specifically interferes with the growth of cancer cells (AMERICAN CANCER SOCIETY, 2015). The objectives of chemotherapy and radiotherapy are to promote the destruction and prevent the proliferation of tumor cells, which are susceptible to death, since they have a higher growth rate than healthy cells (SOARES et al., 2010) . However, these conventional methods also affect the healthy cells, and therefore there is a great effort to develop more selective treatments for the disease, that act directly on the tumor cells, not damaging the healthy cells. Methods using MNPs, photodynamic therapy (PDT), and hyperthermia (HPT) (Figure 9), for example, are considered promising for the fight against cancer, since they present the desired selectivity.

Figure 9. Illustration of cancer treatment by hyperthermia.
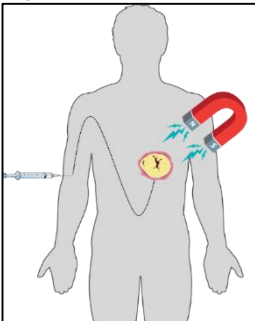
Source: From the author.

The procedure of encapsulating drugs in polymer nanoparticles presents many advantages when compared to the use of drugs in their free form, as the protective effect against drug degradation, controlled or continuous release, possibility of transporting the drug within the target tissue, and reduction of side effects (FELICE et al., 2014; FEUSER et al., 2014; JONG; BORM, 2008; REN et al., 2013). In the systems in question,

NPs have the function of protecting and preventing the aggregation of MNPs (TANG; HASHMI; SHAPIRO, 2013), while the MNPs can guarantee the mobility of the NPs when a magnetic field is applied, allowing the use for the transport of a drug.

The field of nanomedicine, despite being conceptualized as far back as the 1980s, is only transitioning in a broad sense from academic research to drug development and commercialization in the last decades. In oncology, unique structural features of many solid tumors, including hypervasculature, defective vascular architecture, and impaired lymphatic drainage leading to the well-characterized enhanced permeability and retention (EPR) (MATSUMURA; MAEDA, 1986) effect, are key factors in advancing this platform technology. Thus, limitations and challenges both in understanding tumor structural features and correlating them with the technology must be addressed and additional critical data need to be generated before nanotechnology-based drug delivery approaches can be fully realized in clinical use in patients with cancer (PRABHAKAR et al., 2013).

2.7 SIMULTANEOUS ENCAPSULATION OF ANTICANCER DRUGS AND MAGNETIC NANOPARTICLES

In recent years, nanotechnology has been stimulating the development of new medicines and clinical treatments. Currently, it is possible to specifically synthesize and characterize the functional properties of nanoparticles for various applications. Nanoformulations of drugs composed of systemically released small molecules are more effective and less toxic than the same drug used in its free form. This efficacy is attributed to the small size of the molecules, to the modification of pharmacokinetics and their biodistribution (SAIYED; GANDHI; NAIR, 2010).

Magnetic polymer nanoparticles have been considered as an effective system for the treatment of cancer since they contribute to an accurate delivery of the drug at the desired site. The possibility of releasing the drug with a high concentration at a specific site by the influence of a magnetic field can significantly reduce the side effects and increase the therapeutic efficacy (KONERACKÁ et al., 2008). Some studies have been developed regarding the simultaneous encapsulation of drugs and MNPs, in which the encapsulation of indomethacin can be cited (ZÁVIŠOVÁ et al., 2007) and the encapsulation of the anticancer agent taxol (KONERACKÁ et al., 2008), both of which used the

nanoprecipitation technique. Using the technique of miniemulsion polymerization, the work of Feuser et al. (2015b) can be mentioned, which simultaneously encapsulated MNPs and zinc phthalocyanine, an anticancer drug.

2.7.1 Cell uptake

In the treatment of cancer, one of the major issues is the inability for effective penetration of anticancer drugs. Even small molecule drugs can generally penetrate only a few or several cell layers due to the increased abnormalities in both the vasculature and viscosity (FUKUMURA; JAIN, 2008).

A characteristic of various solid tumor types is reduced oxygen availability (hypoxia), which is highly associated with poor vasculature. Although the formation of new blood vessels is induced in the tumor environment, the growth of the cancer cells is faster resulting in insufficient supply of nutrients and oxygen. This phenomenon leads to the development of resistance of tumor cells to chemotherapy and radiotherapy (ANGELOPOULOU et al., 2017). In this context, magnetic nanoparticles' properties can allow nanoparticles to exploit the vasculature and be located to the tumor area through EPR effect and be placed at any tumor site even in the hypoxic zone via application of localized magnetic field gradients (JABR-MILANE et al., 2008; MODY et al., 2014).

Significant improvements in cellular uptake of MNPs into tumor cells was observed by some authors when an external magnetic field was applied. Prijic et al. (2010) synthesized superparamagnetic iron oxide nanoparticles of approximately 12 nm in diameter, composed of an iron oxide core coated with a layer of silica. It was found that the exposure to neodymium-iron-boron magnets (NdFeB) significantly increased the cellular uptake of the material by human melanoma SK-MEL-28 cells, mouse L929 fibroblasts, and human mesothelial MeT-5A cells. Angelopolou et al. (2017) developed hybrids polymer-MNPs consisting of a magnetic iron oxide core and a poly(methacrylic acid)-graft-poly(ethyleneglycol methacrylate) polymeric shell, with an average size of 70 nm. The sodium-glucose transporter protein inhibitor dapagliflozin was incorporated in the material and the application of an external magnetic field gradient increased the uptake of nanoparticles by human lung adenocarcinoma epithelial cells A549.

2.7.2 Controlled release

Biomedical utilization of nanotechnology, which led to the emergence of a new area called "nanomedicine," is an exciting and rapidly advancing field with potentially significant impacts on diagnosis and therapeutics for treatment of human diseases (AMBROGIO et al., 2011; BLANCO et al., 2011; PALIWAL et al., 2011; TAN et al., 2011; VEISEH et al., 2013). Controlled drug release from nanoparticle drug carriers by external stimuli such as temperature, light radiation, electric or magnetic fields, and changes in pH (HRIBAR et al., 2011; KONG et al., 2007; ZHAO et al., 2011) has attracted much attention for its potential in regulating and maintaining drug delivery of a desired therapeutic concentration range at a disease site. Localized, controlled drug release improves the efficacy of the delivered drugs and minimizes toxic side effects (UHRICH; CANNIZZARO, 1999).

Among the applications for the controlled release of drugs, sustained releases of days, weeks or months and releases directed to a specific region (for example a diseased tumor or a blood vessel) are included (GRIFFITH, 2000). Controlled release formulations can be used to reduce the amount of drug required to cause the same therapeutic efficacy in patients. In addition, the use of fewer doses, more effectively, also increases patients compliance (BRAZEL; PEPPAS, 1994).

In various controlled release formulations, immediately upon dispersion in the release medium, a large amount of drug is initially released before the release rates reach a stable profile. This phenomenon is typically called as burst release. Researchers seek to avoid such phenomena because high rates of initial release may lead to concentrations near or above the level of toxicity *in vivo* (JEONG; BAE; KIM, 2000; SHIVELY et al., 1995). In addition, even if there is no negative effect on the patient, this amount of drug is essentially wasted.

Methods of synthesis and storage conditions may explain the burst release. Migration of the drug during the drying and storage stages of the samples may result in heterogeneous drug distributions in the polymer matrix (KISHIDA et al., 1998; MALLAPRAGADA; PEPPAS; COLOMBO, 1997)[8, 11]. In a study of the controlled release of FITC-BSA from polymer matrices based on the PLA mixture with Pluronic, Park et al. (1992a, 1992b) pointed out that the phenomenon of burst observed in several cases was partially due to the formation of pores and cracks in the polymer matrices during its manufacture. This phenomenon is particularly acute when the devices are prepared via solvent

evaporation, as an increase of the organic solvent removal rate causes an increase in the porosity of the matrices (JALIL; NIXON, 1990).

Thorat et al. (2016) encapsulated iron oxide (g-Fe_2O_3-maghemite) nanoparticles within the matrix of (bis(p-sulfonatophenyl)phenylphosphine)-methoxypolyethylene glycol–thiol (mPEG) polymer vesicles using a two-step process for active chemotherapeutic cargo doxorubicin (DOX) loading in cancer theranostics. The simultaneously encapsulated DOX was able to kill cancer cells more efficiently than free DOX *in vitro* without causing toxicity. The material also exhibited enhanced contrast properties that open potential applications for magnetic resonance imaging. Later, Thorat et al. (2017) functionalized superparamagnetic $La_{0.7}Sr_{0.3}MnO_3$ nanoparticles (SPMNPs) with an oleic acid-polyethylene glycol (PEG) polymeric micelle structure, and loaded it with DOX for *in vitro* delivery into cancer cells, obtaining good colloidal stability and biocompatibility due to the micellar structure. The cancer cell death rate was comparable to free DOX, and the counterstrategy of DOX conjugated SPMNPs-induced hyperthermia resulted the cancer cell extinction under *in vitro* conditions.

CHAPTER III

This chapter contains part of the article entitled "Enhanced cellular uptake of superparamagnetic poly(thioether-ester) nanoparticles under an external magnetic field", which was submitted.

3 SYNTHESIS   OF   SUPERPARAMAGNETIC POLY(THIOETHER-ESTER)   NANOPARTICLES   VIA MINIEMULSIFICATION AND SOLVENT EVAPORATION

3.1 INTRODUCTION

Superparamagnetic iron oxide nanoparticles (SPIONs) were first used more than 30 years ago as contrast agents for magnetic resonance imaging (MRI) (WEBB, 2006). Since then, this material have been widely used in a number of applications in the biomedical field (SAHOO et al., 2013; XIE et al., 2015; ZHAO et al., 2014). SPIONs have been to date the only magnetic nanoparticles approved for clinical use and must have, combined, properties of high magnetic saturation, superparamagnetic properties, and biocompatibility for these applications. The dual-functional nature of magnetic nanoparticles (MNPs) as both imaging agent and a carrier for target specific pharmaceutics under a magnetic field gradient has made them attractive delivery agents *in vitro* and *in vivo*. The simultaneous application of MNPs with highly cytotoxic drugs can attenuate side effects when the two are combined due to the targeted delivery (DAVE; GAO, 2009; MACDONALD et al., 2010; SAIYED; GANDHI; NAIR, 2010).

The use of polymeric nanoparticles for drug delivery results in higher and localized concentrations of the drug in a specific site, reducing the toxic effects on healthy cells or tissues, providing a strategy for the diagnosis and treatment of diseases. Natural and synthetic biodegradable polymers have prospective applications in drug delivery because they can be breakdown into smaller molecules under specific biological stimuli (MACHADO; SAYER; ARAUJO, 2017). The thiol-ene polymerization is a promising tool for synthesizing polymeric nanoparticles (JASINSKI et al., 2014, 2016) with potential for biomedical applications. Innovative biomaterials are arising from this technique due to the interest on its unique attributes, including mild reaction conditions, fast reaction rates, and without formation of by-products (JASINSKI et al., 2014). Thereby, nanoparticles will have the function of protecting and preventing the

aggregation of MNPs, in the systems in question (TANG; HASHMI; SHAPIRO, 2013). On the other hand, MNPs will be able to guarantee the mobility of the polymeric nanoparticles when a magnetic field is applied, allowing the use for drug transportation (GULIN-SARFRAZ et al., 2014; NOWICKA et al., 2013; QIU et al., 2017).

A large number of studies have been developed regarding the encapsulation of MNPs in polymeric colloidal particles, applying methods such as emulsion polymerization (M. VAN HERK; LANDFESTER, 2010), inverse miniemulsion polymerization (ROMIO et al., 2013) and direct polymerization (HE et al., 2009; LANDFESTER; RAM REZ, 2003; STAUDT et al., 2013). Some studies have also shown a significant improvement in cellular uptake of MNPs into tumor cells when an external magnetic field was applied (ANGELOPOULOU et al., 2017; PRIJIC et al., 2010).

Drug nanocarriers with magnetic properties are a promising material for biomedical applications. Additionally, environmentally friendly materials have been heavily targeted in recent decades due to crescent concern about environmental problems. Thus, this chapter presents the synthesis and characterization of MNPs encapsulated in poly(thioether-ester) (PTEe) nanoparticles via the miniemulsification and solvent evaporation method, given that PTEe was synthesized via thiol-ene miniemulsion polymerization using a fully renewable α,ω-diene monomer obtained from 10-undecenoic acid and 1,3-propanediol, both derived from castor oil. Also, the *in vitro* cytotoxicity and cellular uptake of MNPs-PTEe nanoparticles in human cervical cancer (HeLa) cells were evaluated under an external magnetic field.

3.2 MATERIALS AND METHODS

3.2.1 Materials

The renewable monomer and the PTEe nanoparticles were prepared with 10-undecenoic acid (Sigma-Aldrich, 98%), 1,3-propanediol (Sigma-Aldrich, 99.6%), p-toluenesulfonic acid monohydrate (Sigma-Aldrich, 98.5%), sodium dodecyl sulfate (SDS, Vetec), azobisisobutyronitrile (AIBN, Vetec, 98%) and 1,4-butanedithiol (Sigma-Aldrich, >97%). The synthesis of the magnetic nanoparticles (MNPs) involved the following reagents: ferrous sulfate ($FeSO_4 \cdot 4H_2O$), iron (III) chloride hexahydrate ($FeCl_3 \cdot 6H_2O$), ammonium hydroxide (99%) and oleic acid (OA), all purchased from Vetec. The

encapsulation of the MNPs and the *in vitro* assayss were made using the following: sodium dodecyl sulfate (SDS), NaH_2PO_4 (sodium phosphate monobasic) and Na_2HPO_4 (sodium phosphate dibasic), purchased from Vetec, were used as surfactant and buffers, respectively; lecithin (Alpha Aesar); dichloromethane (DCM, Panreac, 99,8%) was used as solvent. Distilled water was used throughout the experiments.

3.2.2 Renewable monomer and poly(thioether-ester) (PTEe) nanoparticles preparation

The synthesis of the renewable monomer, 1,3-propylene diundec-10-enoate, and PTEe via thiol-ene miniemulsion polymerization was the same as described by Cardoso et al. (2017). PTEe samples were lyophilized for further use.

10-Undecenoic acid (50.0 g, 0.27 mol), 1,3-propanediol (8.4 g, 0.11 mol), p-toluenesulfonic acid (3 g, 0.0157 mol) and toluene (200 mL) were added to a round-bottomed flask equipped with a magnetic stirrer and a Dean-Stark apparatus. The resulting mixture was heated to reflux and water was collected as the reaction proceeded. Once the reaction was completed, the reaction mixture was allowed to cool down. After removing the toluene under reduced pressure, the residue was filtered through a short pad of basic aluminium oxide with hexane as eluent. Hexane was removed and the crude product was dissolved in diethyl ether (200 mL) and washed two times with water (200 mL). The organic fraction was dried over anhydrous $MgSO_4$ and the solvent removed under reduced pressure.

For the miniemulsion reactions, the aqueous phase was prepared mixing water (10 mL) and 0.019 wt. % of SDS as surfactant. The mixture was let stirring until complete surfactant solubilization. The organic phase was prepared mixing the α,ω-diene monomer (1.0 g) and 1 mol % of the organic-soluble initiator AIBN (relative to BDT) under magnetic stirring until complete initiator solubilization. The aqueous phase was added to the organic phase and, after 10 min of vigorous magnetic stirring (500 rpm), a macroemulsion was obtained. Then 0.29 mL of BDT was added to the system (1:1 dithiol-to-diene molar ratio) with a micropipette and the mixture was let under mild magnetic stirring (250 rpm) for 5 min. The final emulsion was sonicated for 2 min (10 s on, 2 s off) with amplitude of 60%, using a Fisher Scientific Sonic Dismembrator model 500 and 1/2" tip. An ice bath was used to reduce the temperature increase during the sonication.

3.2.3 Magnetic nanoparticles (MNPs) preparation

The MNPs coated with oleic acid (MNPs-OA) were prepared according to the method used by Feuser et al. (2015a). The MNPs were synthesized by the method of coprecipitation in aqueous medium. First, $FeSO_4 \cdot 7H_2O$ and $ClFe_3 \cdot 6H_2O$ were solubilized in distilled water in the 1:1 molar ratio. Subsequently, NH_4OH was added controlling the initial (1) and final (10) pH of the reaction, using room temperature and a stirring speed of 700 rpm. In the second step, OA was added to stabilize the MNPs. After stabilizing, the material was washed with acetone to remove excess of OA and then the sample was centrifuged and washed several times until the excess of OA was completely removed.

3.2.4 Superparamagnetic poly(thioether-ester) (MNPs-PTEe) nanoparticles preparation

The encapsulation of MNPs in the PTEe nanoparticles was performed by the method of miniemulsification and solvent evaporation. The aqueous phase was prepared mixing water (7 g) and the surfactant SDS (0.5 wt. %) and the mixture was let stirring until complete surfactant solubilization. The organic phase was prepared mixing pre-formed PTEe (40 mg), lecithin as surfactant (15 mg) and dichloromethane as solvent (0.6 g), plus 0.6 g of DCM with 15 mg of the MNPs containing approximately 27% of OA. The organic phase was added to the aqueous phase at the beginning of the sonication step. Sonication occurred for 3 min (20 s on, 10 s off) with amplitude of 70% (Fisher Scientific Sonic Dismembrator model 500 and a 1/2" tip). An ice bath was used to reduce the temper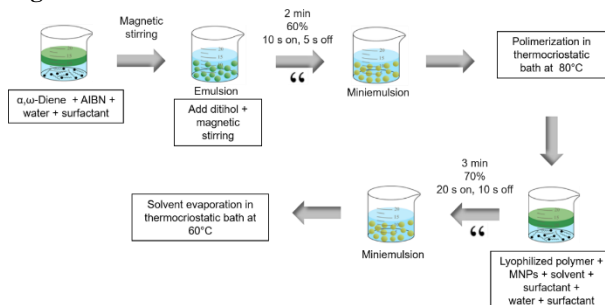ature increase during the sonication. The miniemulsion was left in a thermostatic bath with a temperature of 60 °C until complete solvent evaporation. The preparation of the polymer, as well as the encapsulation of MNPs is illustrated in Figure 10.

Figure 10. Production of MNPs-PTEe scheme.

Source: From the author.

3.2.5 Nanoparticles characterization

3.2.5.1 Transmission Electron Microscopy (TEM)

Particle morphology characterization was performed by Transmission Electron Microscopy using a JEM-1011 TEM (100 kV). For this analysis, the sample was diluted in distilled water down to 0.01% of solids content and one single drop was placed on a carbon-coated copper grid. Then the grid was dried under room conditions overnight. The analysis was carried out in the Central Electron Microscopy Laboratory (LCME) of the Federal University of Santa Catarina.

3.2.5.2 Dynamic Light Scattering (DLS)

Particle size (Dp), polydispersity index (PdI) and the surface charge of the nanoparticles were measured by dynamic light scattering (DLS) using a Malvern Zetasizer Nano ZS analyzer. The surface charge of the nanoparticles was investigated through zeta potential measurements. For both the analyses, all samples were analyzed three times at room temperature (25 °C), from which the average and standard deviation (SD) were calculated. The analyses were carried out in the Laboratory of Processes Control (LCP) and in the Interdisciplinary Laboratory for the Development of Nanostructures (LINDEN), both situated in the Department of Chemical Engineering and Food Engineering of the Federal University of Santa Catarina.

3.2.5.3　Thermogravimetric analysis (TGA)

Polymeric nanoparticles were characterized through thermogravimetric analysis (TGA, STA 449 F3 Jupiter, NETZSCH) to determine the concentration of MNPs incorporated. Approximately 10 mg of each sample was weighed in a platinum pan and the runs were carried under nitrogen atmosphere at a heating rate of 10 °C/min between 20 °C and 700 °C. The amount of MNPs incorporated in the PTEe nanoparticles was obtained taking the difference between the percentage of MNPs added to the initial formulation and percentual residue at the end of the analysis. The analysis was carried out in the Laboratory of Processes Control (LCP), situated in the Department of Chemical Engineering and Food Engineering of the Federal University of Santa Catarina.

3.2.5.4　Fourier Transform Infrared Spectroscopy (FTIR)

Chemical characterization was performed by a Fourier Transform Infrared Spectroscopy (FTIR) spectrometer (IRPrestige21, from Shimadzu), using the KBr pellets method. The spectra of the samples were taken in the region of wavelength between 400 and 4000 cm^{-1}. The analysis was carried out in the Laboratory of Processes Control (LCP), situated in the Department of Chemical Engineering and Food Engineering of the Federal University of Santa Catarina.

3.2.5.5　Vibration Sample Magnetometer (VSM)

The VSM allows us to obtain information about the magnetic properties of a given material and to classify it according to its magnetic properties, being it ferrimagnetic, ferromagnetic or superparamagnetic. The magnetic properties were measured at 300 K using an EV9 (MicroSense) electromagnet vibrating sample magnetometer. Samples were prepared by placing a small amount of the material, with a known mass, inside a glass capsule which was clamped by a quartz tube and fixed vertically on two coils. The applied magnetic field was varied between 20 to -20 KOe and measurements were performed at room temperature. The analysis was performed in the Multi-user X-Ray Diffraction and VSM Laboratory, from the Department of Physics of the Federal University of Santa Catarina.

3.2.6   Cell viability assay – HeLa cells

The cells were grown in MEM medium containing 10% FBS, 100 µg/mL penicillin/streptomycin and maintained at culture conditions (37 °C in a humidified atmosphere with 5% CO_2). The cells were seeded at 1×10^4 cells/well in a 96-well plate and incubated for 30 min at different concentrations (10, 30, 60 and 100 µg/mL) of MNPs-PTEe nanoparticles (resuspended in MEM) with and without magnetic field (neodymium iron boron magnet). Magnets, with a magnetic field strength of 1500 Oe were placed under the plate wells (GULIN-SARFRAZ et al., 2014). After incubation the cells were washed twice with PBS. Next, 200 µL of MTT (0.5 µg/mL) were added in each well and the cells were incubated for 3 h. After the incubation period, the MTT was removed and 200 µL of DMSO was added to dissolve the formazan crystals. Lastly, the absorbance was measured at 550 nm using a Loccus LM-96 microplate reader. The experiments were performed in triplicate with four wells for each condition. The results were expressed as the percentage of viable cells in comparison to the control group (untreated cells).

3.2.7   Fluorescence analysis

MNPs-PTEe nanoparticles labeled with 6-coumarin were used for cellular uptake studies by fluorescence images. HeLa cells (1×10^4) were seeded in a 24-well black-walled microplate and maintained for 24 h at culture conditions. The culture was then exposed to the MNP-PTEe nanoparticles (10 µg/mL) and incubated for 10 min or 30 min, with and without an external magnetic field. After the incubation, the magnets were removed and cells were washed three times with PBS to remove all non-internalized nanoparticles from the cell surface. Next, the nuclei of the cells were stained with Hoechst 33342 (3.5 µg/mL), incubated (PBS 7.4) for 5 min and the images were analyzed. All the analyses were performed with an inverted microscope Nikon Eclipse Ti-U equipped with a fluorescent lamp and using the suitable filter for each fluorophore.

3.3 RESULTS AND DISCUSSION

3.3.1   Nanoparticles characterization

Figure 11 displays TEM images of the empty PTEe (A) and the MNPs encapsulated in the PTEe nanoparticles (B) and (C), all of them

obtained by the method of miniemulsification and solvent evaporation. It can be noticed that nanoparticles have spherical morphology and diameter around 150 nm. The PTEe nanoparticles degraded when exposed to the electron beam during TEM analysis. The degradation is more intense for longer exposition times and it was used to expose MNPs contained inside the PTEe nanoparticles, as can be observed in Figures 1B and C, in which the MNPs are attributed to the darker points.

Figure 11. TEM analyses of nanoparticles of empty PTEe (A) and MNPs-PTEe (B) and (C).
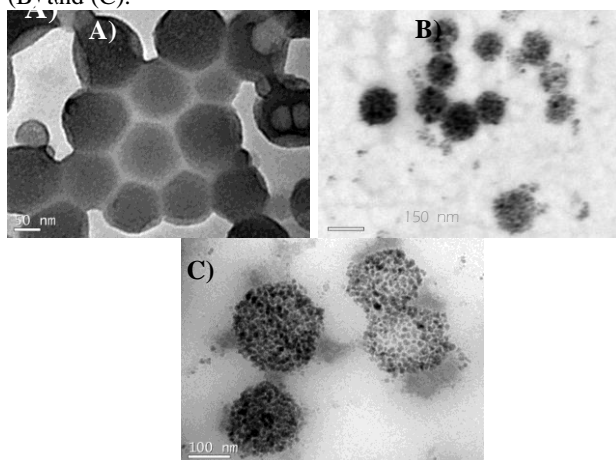
Source: From the author.

DLS results corroborate with the TEM analysis, since the particles size are in the same range and PdI values lower than 0.2 indicate that the samples have a narrow size distribution, as shown in Table 2. Both morphology and particle size distribution have biological implications on cellular uptake and biological processes (DANHIER; FERON; PRÉAT, 2010; HE et al., 2010). According to Moghimi et al. (2001), nanoparticles diameter should be between 120 and 200 nm to avoid sequestration and extravasation to the tissues in order to maximize the cellular uptake. The zeta potential is an important characteristic of the nanoparticles because it provides information about the colloidal stability, as well as the cellular uptake and trafficking pathways (HARUSH-FRENKEL et al., 2008). Zeta potential values of approximately −40 mV at physiological pH indicates good stability without formation of aggregates, contributing to a higher colloidal

stability (ANTONIETTI; LANDFESTER, 2002; PRIJIC et al., 2010). However, slight surface charge differences and different cell lines have significant implications in the cellular uptake of nanoparticles (HE et al., 2010). The negative charges in the particles analyzed are associated with the presence of surfactants, such as the SDS, adsorbed on the nanoparticle surface (FEUSER et al., 2014).

Table 2. Intensity mean diameter of nanoparticles (Dp), polydispersity index (PdI) and zeta potential in pH 7.

Sample	Dp (nm)	PdI	Zeta Potential (mV)
empty PTEe	143 ± 4	0.20 ± 0.03	-42 ± 3
MNPs-PTEe	149 ± 6	0.16 ± 0.02	-46 ± 2

$\pm$ Mean standard deviation of n = 3 determinations
Source: From the author.

The absorption bands of the functional groups present in the samples could be verified by FTIR analyses, which are shown in Figure 12. The band at approximately 580 cm^{-1} corresponds to Fe-O, which is attributed to the MNPs (FEUSER et al., 2015a; PATIL et al., 2014; SHETE et al., 2014; XIE et al., 2015) and is displayed both in the PTEe-MNPs nanoparticles and in the MNPs-OA spectra. In the empty PTEe nanoparticles spectrum, it can be noticed that there is no peak correspondent to C=C double bonds at 1640 cm^{-1}, indicating absence of residual diene monomer. Additionally, the presence of C-S-C stretching at 720 cm^{-1} can be observed, evidencing the addition of thyil radicals across the double bonds of the diene (CARDOSO et al., 2017). These characteristics can be observed both in the empty PTEe and in the MNPs-PTEe nanoparticles samples.

The thermal decomposition of MNPs-PTEe nanoparticles was evaluated by thermogravimetry and the result is displayed in Figure 13. There was no mass loss between 0 and 100 °C, which can indicate the material is free of volatile impurities and water (LANDFESTER; RAM REZ, 2003; SHETE et al., 2014). The mass loss was gradual (200-430 °C) with biggest mass loss occurring in the temperature range of 350-430 °C, approximately. The PTEe nanoparticles and oleic acid coated in MNPs were completely degraded after reaching about 430 °C. The residual concentration of approximately 10% for the MNPs-PTEe nanoparticles corresponds to the MNPs, which represents an incorporation higher than 99 %, considering that the magnetite used in the

formulation contained an amount of approximately 28% of OA, that is completely degraded between 200 and 430 °C (LANDFESTER; RAM REZ, 2003)

Figure 12. FTIR analyses of PTEe, MNPs-PTEe nanoparticles and MNPs coated with OA.
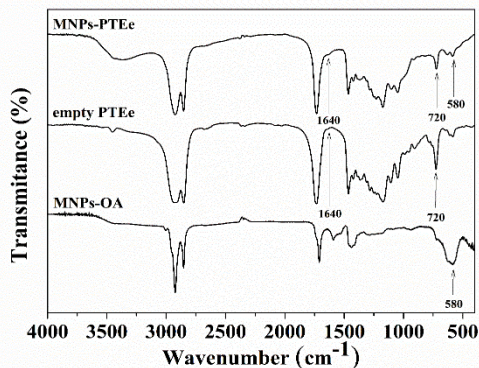
Source: From the author.

Figure 13. TGA analysis of MNPs coated with OA and MNPs-PTEe nanoparticles obtained.
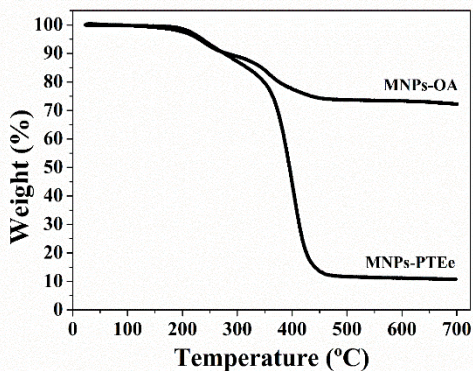
Source: From the author.

The magnetic properties of MNPs coated with oleic acid (OA) and MNPs-PTEe nanoparticles were obtained by VSM. Figure 14 illustrates the magnetization curves at room temperature. The MNPs coated with OA and MNPs-PTEe nanoparticles presented typical superparamagnetic behavior, as shown by the absence of coercivity and

remanence magnetization, and high saturation magnetization (FEUSER et al., 2014; SOARES et al., 2016). The superparamagnetic proprieties are very important for their application in biomedical field. In this way, without the presence of an external magnetic field, their overall magnetization value is randomized to zero, avoiding interactive behavior of the particles when there is no an applied magnetic field (MODY et al., 2014).

Figure 14. VSM analyses of MNPs coated with OA and MNPs-PTEe nanoparticles.
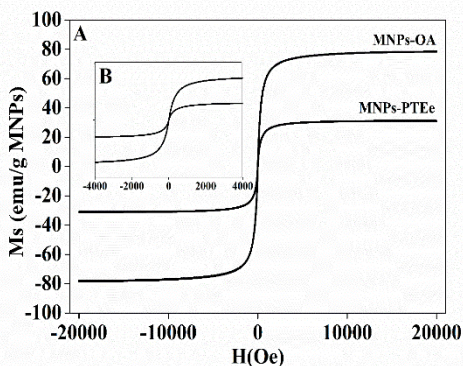
Source: From the author.

The magnetic behavior can also be observed in Figure 15. MNPs-PTEe nanoparticles were well dispersed (pH 7.4) without the presence of magnetic field (A) and they were attracted to the magnet when an external magnetic field was applied (B). The results show that the saturation magnetization presented by MNPs-PTEe nanoparticles is sufficient to be directed to a specific target.

Figure 15. MNPs-PTEe sample without application of magnetic field (A) and with magnetic field application (B).
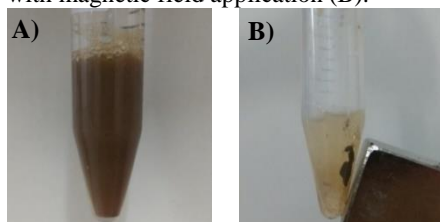
Source: From the author.

3.3.2 Cell viability assay

The results of the cell viability assays of MNPs-PTEe nanoparticles incubated for 30 min with MNPs-PTEe nanoparticles, with and without magnetic field application on HeLa cells, are displayed in Figure 15. The results showed that the MNPs-PTEe nanoparticles under the presence of an external magnetic field did not present any cytotoxic effect on HeLa cells in all concentrations tested (no significant difference). These results are very important for the use of these nanoparticles as drug carriers.

Figure 16. Cell viability assay of MNPs-PTEe nanoparticles with and without field magnetic application at different concentrations. Significant differences are shown (one-way ANOVA followed by post-test Bonferroni's).
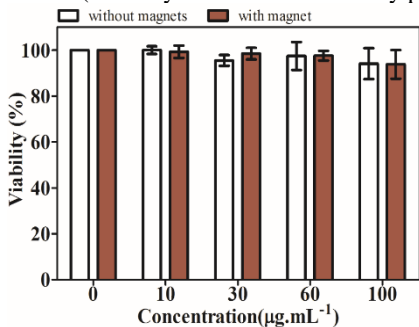
Source: From the author.

3.3.3 Cellular uptake of MNPs-PTEe nanoparticles under an external magnetic field

Magnetic nanoparticles as potential delivery systems must be able to be internalized into the cells. MNPs-PTEe nanoparticles were labeled with 6-coumarin, thus the internalization was measured by fluorescence microscopy analysis and the results are shown in Figures 17 and 18. As it can be observed from Figure 17, MNPs-PTEe nanoparticles incubated for 10 or 30 min in the presence of an external magnetic field (17D, E and F) presented higher cellular uptake than the nanoparticles without the application of an external magnetic field (17B and C).

The quantification analysis of fluorescence was evaluated by mean pixel intensity. As it can be seen in Figure 16, when the MNPs-PTEe nanoparticles were incubated for 10 or 30 min in the presence of an external magnetic field, the cellular uptake was up to three times higher

than MNPs-PTEe nanoparticles incubated without magnetic field. Similar result was observed by Yang and coworkers (2014), in which the uptake of MNPs-PEI (polyethyleneimine) nanoparticles by human breast cancer cells was significantly higher in the presence of an external magnetic field, resulting in a higher efficiency in the delivery of antitumor drugs and reducing the toxic effects on healthy cells or tissues.

Figure 17. Cellular uptake of MNPs-PTEe nanoparticles labeled with 6-coumarin at a concentration of 10 µg.mL-1. Hela cells were incubated for 10 and 30 min at 37 °C: (A) control group (only cells), (B, C) without magnetic field and (D, E, F) with magnetic field.
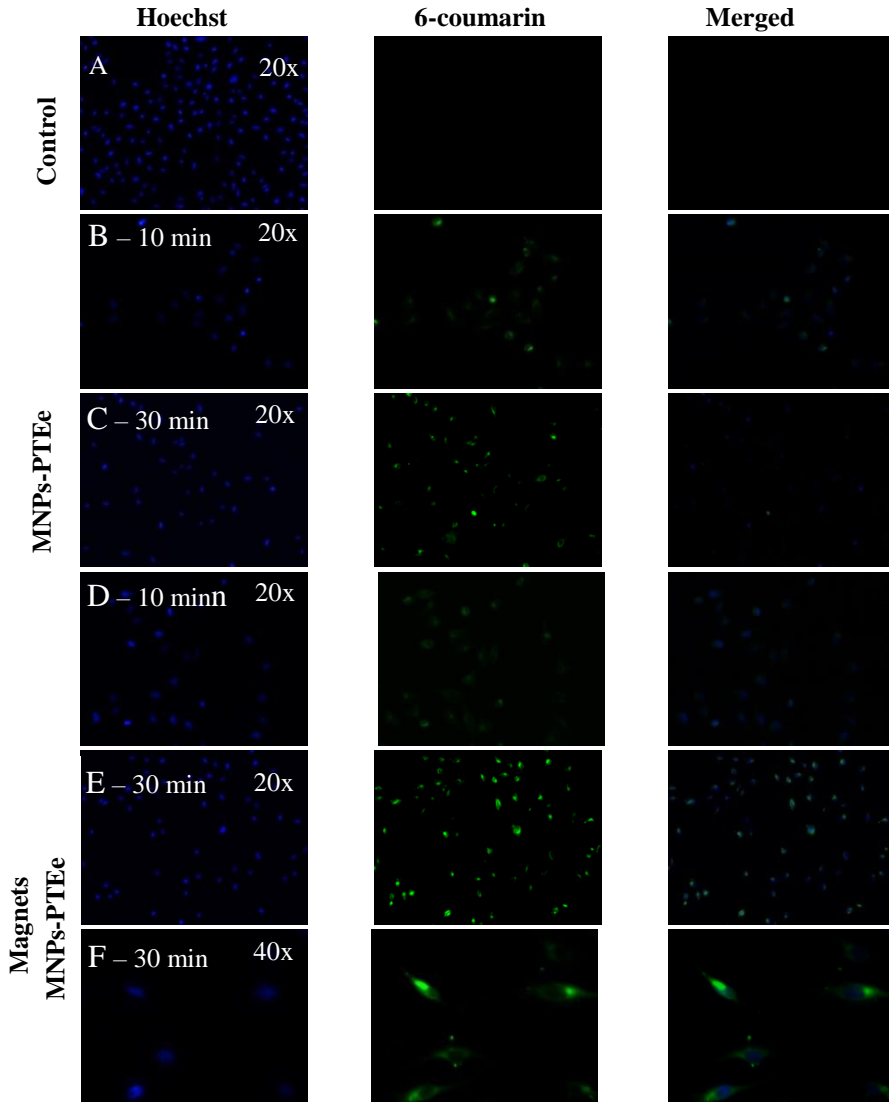
Source: From the author.

Figure 18. Quantification of fluorescence intensity by ImajeJ software. HeLa cells were incubated for 10 and 30 min with MNPs-PTEe nanoparticles labeled with 6-coumarin at concentration of 40 µg/mL with and without magnetic field application. (*p < 0.01) using one-way ANOVA followed by Tukey test.
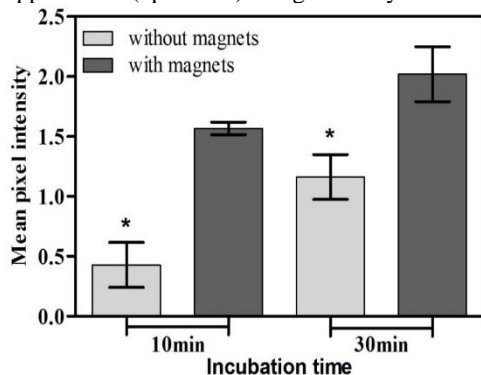
Source: From the author.

3.4 CONCLUSION

Magnetic nanoparticles coated with oleic acid were efficiently incorporated in poly(thioether-ester) nanoparticles by the miniemulsification and solvent evaporation method. As a result, MNPs-PTEe nanoparticles with spherical morphology, average diameter around 150 nm, narrow average size distribution, and superparamagnetic properties were obtained. The nanoparticles did not exhibit cytotoxicity according to the results of the cell viability assays under or not the presence of an external magnetic field. Moreover, the fluorescence analysis results showed that the application of a magnetic field increased the cellular uptake of MNPs-PTEe nanoparticles on HeLa cells up to three times. In this way, these results demonstrate that MNPs-PTEe obtained by miniemulsification and solvent evaporation a could be applied in therapies such as hyperthemia or as drug carriers for the treatment of cancer.

CHAPTER IV

4 SIMULTANEOUS ENCAPSULATION OF MNPs AND 4-NITROCHALCONE IN PTEe NANOPARTICLES VIA MINIEMULSIFICATION AND SOLVENT EVAPORATION

4.1 INTRODUCTION

Nowadays, it is unquestionable that cancer is a public health problem. It is one of the leading causes of morbidity and mortality in the world, second only to cardiovascular disease. In 2015, it was responsible for 8.8 million deaths, and this number is expected to grow about 70% over the next two decades (STEWART; WILD, 2014). The greatest difficulty during cancer treatments is to destroy the tumor cells without affecting the healthy tissue in their surroundings, which happens in conventional therapies such as chemotherapy and radiotherapy. Therefore, there is a great effort to develop more selective methods for the treatment of this disease.

Polymeric nanoparticles (NPs) have been considered as an effective system for cancer treatment since they contribute to a precise drug delivery at the desired region of the body. Consequently, the toxic effects are reduced on healthy cells or tissues, providing a novel strategy in the treatment of this disease (KONERACKÁ et al., 2008). Magnetic nanoparticles (MNPs) have been widely used in a number of applications in the biomedical field, as it was already mentioned. In the case of cancer treatments, the possibility of releasing the drug in high concentrations at a specific spot influenced by an external magnetic field can also reduce side effects and increase therapeutic efficiency (KONERACKÁ et al., 2008).

Chalcones are part of a select group of chemical compounds associated with various pharmacological activities. They are polyphenolic compounds which belong to the family of the flavonoids and can be found in several edible plants as metabolic precursors of other flavonoids and isoflavonoids. Epidemiologic studies suggest that the ingestion of flavonoids can reduce the risk of breast, colon, lung, prostate and pancreas tumors (PRAKASH et al., 2013). The antioxidant properties, cytostatic effects on tumorigenesis and the ability to inhibit a wide variety of enzymes, led the researchers to consider chalcones as potential anticarcinogens (SKIBOLA; SMITH, 2000). The chalcones can

act both through the extrinsic and intrinsic pathways of cell apoptosis, preventing tumor evolution (LIU et al., 1996).

Some studies have been developed with the simultaneous encapsulation of drugs and MNPs using techniques such as nanoprecipitation (KONERACKÁ et al., 2008; ZÁVIŠOVÁ et al., 2007) and miniemuslsion polymerization (FEUSER et al., 2015b). The simultaneous encapsulation of 4-nitrochalcone (4NC), an anticancer drug, and MNPs in the same system with the possibility of a controlled release and the minimization of side effects could be a promising new option for cancer treatment. Therefore, the main objective of the work presented in this chapter was the synthesis and characterization of 4NC and MNPs loaded PTEe via miniemulsification and solvent evaporation. *In vitro* release profile and hyperthermia tests were also performed.

4.2 MATERIALS AND METHODS

4.2.1 Materials

The renewable monomer and the PTEe nanoparticles were prepared with 10-undecenoic acid (Sigma-Aldrich, 98%), 1,3-propanediol (Sigma-Aldrich, 99.6%), p-toluenesulfonic acid monohydrate (Sigma-Aldrich, 98.5%), sodium dodecyl sulfate (SDS, Vetec), azobisisobutyronitrile (AIBN, Vetec, 98%) and 1,4-butanedithiol (Sigma-Aldrich, >97%). The synthesis of the magnetic nanoparticles (MNPs) involved the following reagents: ferrous sulfate ($FeSO_4 \cdot 4H_2O$), iron (III) chloride hexahydrate ($FeCl_3 \cdot 6H_2O$), ammonium hydroxide (99%) and oleic acid (OA), all purchased from Vetec. The encapsulation of the MNPs and 4-nitrochalcone, and the *in vitro* assays were made using the following: sodium dodecyl sulfate (SDS), NaH_2PO_4 (sodium phosphate monobasic) and Na_2HPO_4 (sodium phosphate dibasic), purchased from Vetec were used as surfactant and buffers, respectively; lecithin (Alpha Aesar); 4-nitrochalcone (4NC, Sigma-Aldrich); dichloromethane (DCM, Panreac, 99,8%) was used as solvent. Distilled water was used throughout the experiments.

4.2.2 Encapsulation of MNPs and 4NC in poly(thioether-ester) nanoparticles

The MNPs-OA preparation, the synthesis of the renewable monomer, and the synthesis of empty PTEe NPs were made as described in Chapter 3, sessions 3.2.2 and 3.2.3.

The simultaneous encapsulation of MNPs and 4NC in the PTEe NPs was performed by miniemulsification and solvent evaporation, as described in the previous chapter, but adding 4NC in the organic phase. The aqueous phase was prepared mixing water (7 g) and the surfactant SDS (0.5 wt. %) and the mixture was let stirring until complete surfactant solubilization. The organic phase was prepared mixing the pre-formed poly(thioether-ester) NPs (40 mg), lecithin as the surfactant (15 mg) and dichloromethane as the solvent (1.8 g) divided in two different solutions: 0.6 g of DCM with 15 mg of the MNPs, which contained approximately 27% of OA, and 0.6 g of a solution of 1 mg 4NC/g DCM. The organic phase was added to the aqueous phase at the beginning of the sonication step. Sonication occurred for 3 min (20 s on, 10 s off) with an amplitude of 70% (Fisher Scientific Sonic Dismembrator model 500 and a 1/2" tip). An ice bath was used to reduce the temperature increase during the sonication. The miniemulsion was left in a thermostatic bath at 60 °C until complete solvent evaporation.

4.2.3 4NC calibration curve

To quantify the concentration of 4NC in the samples, a calibration curve was previously elaborated, in which standard solutions containing known concentrations of the drug were analyzed at the wavelength 324 nm, being determined by scanning in a spectrophotometer (Hitachi, U-1900) in the range of 190 to 400 nm. The analytical curve was obtained by relating the concentration values of 4NC (from 0.5 to 9.5 μg/mL) on the axis of the abscissa (x), with the values for the concentration, on the axis of the ordinates (y). Dilutions were performed with DMSO and Equation 1 was obtained.

$$Abs = (0.1068 \times C_{4NC}) - 0.0166 \tag{1}$$

Where *Abs* is the absorbance and C_{4NC} is the concentration of 4NC (μg/mL). The equation follows the correlation coefficient $R^2 = 0.999$. This

experiment was carried out in the Laboratory of Processes Control (LCP), situated in the Department of Chemical Engineering and Food Engineering of the Federal University of Santa Catarina.

4.2.4 Characterization

Particle size, polydispersity index, surface charge, thermogravimetric analysis, chemical characterization, hysteresis loops measurements, and morphology characterization of the nanoparticles were performed following the procedure described in Chapter 3, session 3.3.5.

The 4NC encapsulation efficiency (EE%) was determined by UV-VIS spectrophotometry. The amount of 4NC present in the nanoparticles was determined by ultracentrifugation of 500 μL of the latex in an eppendorf coupled to an Amicon Ultra 0.5 filter (Millipore®, 100 KDa - 100,000 NMWL) for 30 min at 13.300 rpm. An aliquot of the supernatant was diluted in a ratio of 1:20 in DMSO and transferred to a cuvette (1 cm) for analysis. The 4NC concentrations were measured at 324 nm using the calibration curve with different concentrations of 4NC dispersed in DMSO since the coefficient of determination (R^2) exceeded 0.999, with excellent linearity. The experiments were conducted in triplicate at the Laboratory of Processes Control (LCP), situated in the Department of Chemical Engineering and Food Engineering of the Federal University of Santa Catarina.

4.2.5 *In vitro* 4NC release profile

The *in vitro* release profile was adapted from the method described by Ricci-Junior and Marchetti (2006). Lyophilized samples of MNPs+4NC PTEe (10 mg) were weight and added to 15 mL of the receptor medium, composed of PBS (pH 7.4) and 0.5% wt of SDS. This experiment was also carried out in distilled water with 0.5% SDS and pH 6.0 in order to simulate the tumor cells environment. The suspension was continuously stirred (100 rpm) and the temperature was maintained at 37 °C in a thermostatically controlled water bath. At given time intervals, samples of 2 mL were withdrawn and centrifuged at 13.300 rpm for 5 min. The drug release in the receptor medium was quantified by spectrophotometry at the wave length of 324 nm. The experiment was carried in duplicate. The release profile was obtained by associating the percentage of drug release with time. The release data were fitted using

the zero order, first order, Higuchi and Korsmeyer-Peppas mathematical models described by Costa and Lobo (2001).

4.3 RESULTS AND DISCUSSION

4.3.1 Nanoparticles characterization

Table 3 shows the nanoparticles mean diameter (Dp), polydispersity index (PDI) and zeta potential obtained by DLS, besides the encapsulation efficiency (EE%). Formulations exhibited Dp between 118 and 149 nm approximately, with low polydispersity indexes. Both morphology and particle size distribution have biological implications on cellular uptake and biological processes (DANHIER; FERON; PRÉAT, 2010; HE et al., 2010). Therefore, it is important that these parameters did not suffer great impact with the encapsulation of 4NC.

Free 4NC and 4NC encapsulated in PTEe nanoparticles, alone or simultaneously with the MNPs, have similar spectroscopic behavior, with maximum wavelength at 324 nm. The 4NC was encapsulated alone in PTEe nanoparticles and simultaneously with MNPs. Both formulations presented encapsulation efficiencies higher than 90 %.

Table 3. Intensity mean diameter of nanoparticles (Dp); polydispersity index (PdI); zeta potential in pH 7 and encapsulation efficiency (EE%).

Sample	Dp (nm)	PdI	Zeta Potential (mV)	EE (%)
empty PTEe	143 ± 4	0.20 ± 0.03	-42 ± 3	-
4NC-PTEe	132 ± 2	0.21 ± 0.07	-48 ± 3	93 ± 4
MNPs-PTEe	149 ± 6	0.16 ± 0.02	-46 ± 2	-
MNPs+4NC-PTEe	118 ± 6	0.21 ± 0.07	-49 ± 2	96 ± 3

$\pm$ Mean Standard deviation of n = 3 determinations
Source: From the author.

Figure 19 shows TEM images of the different nanoparticles synthesized. It can be noticed that all the nanoparticles have nanometric size, spherical morphology and narrow size distribution, corroborating with the DLS analysis. It is possible to observe the magnetite nanoparticles encapsulated, being the MNPs attributed to the darker

points in the images (C and D). As it can be seen in the TEM images in Figure 1C and D, PTEe nanoparticles contained several MNPs.

Figure 19. TEM analyses of nanoparticles of empty PTEe (A), 4NC-PTEe (B), MNPs-PTEe (C) and MNPs+4NC-PTEe (D).
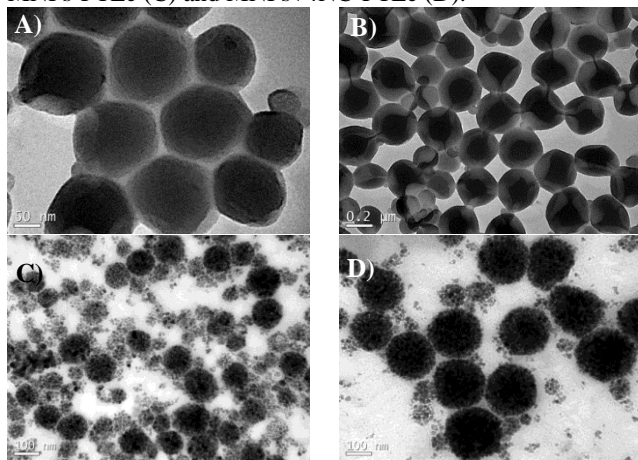
Source: From the author.

The presence of the absorption bands of the functional groups present in the samples could be verified by FT-IR analyses, which are displayed in Figure 20. The results were very similar to the ones observed at Chapter III. As in the previous analyses, it was possible to identify the main bands corresponding to the MNPs and to the polymer in the new MNPs+4NC PTEe sample. The free 4NC FT-IR spectra shows characteristic absorption bands at 2918 and 2848 cm^{-1} (CH stretch), 3075 cm^{-1} (asymmetric CH stretch), 1660 cm^{-1} (C=O stretch), 1608 and 1594 cm^{-1} (C=C stretch), 1512 cm^{-1} (NO$_2$ stretch), 1409 cm^{-1} (CH deformation), 1340 cm^{-1} (C=C-NO$_2$), 1221 and 1106 cm^{-1} (structural C-C), 1013 cm^{-1} and lower (aromatic CH deformation) (PATIL et al., 2006; SIGMA-ALDRICH, 2018; SILVERSTAIN; WEBSTER; KIEMLE, 2005). The comparison between the FT-IR spectra of MNPs+4NC PTEe and free 4NC suggests that there is no significant interaction between the drug and the polymer. It shows that 4NC is located in the polymeric matrix, i.e. it is molecularly dispersed, and not at the surface (FEUSER et al., 2015b).

Figure 20. FTIR analyses of the MNPs-OA and the PTEe nanoparticles obtained.
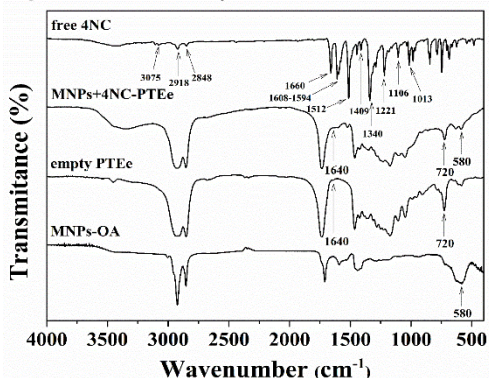
Source: From the author.

Thermogravimetry analyses were performed to evaluate the thermal decomposition of 4NC+MNPs PTEe as well as the amount of MNPs incorporated in the formulations. In this case also, encapsulation of 4NC did not affect the results. As it can be seen in Figure 21, the thermal decomposition of 4NC+MNPs PTEe has a similar behavior compared to the MNPs-PTEe, so the second is not displayed in the graph. The residual concentration of approximately 10 % for the 4NC+MNPsPTEe nanoparticles represents an incorporation of magnetite higher than 99 %, considering that the material used in the formulation had 28 % of OA remaining (LANDFESTER; RAM REZ, 2003).

Figure 21. TGA analyses of MNPs-OA and MNPs+4NC PTEe nanoparticles obtained.
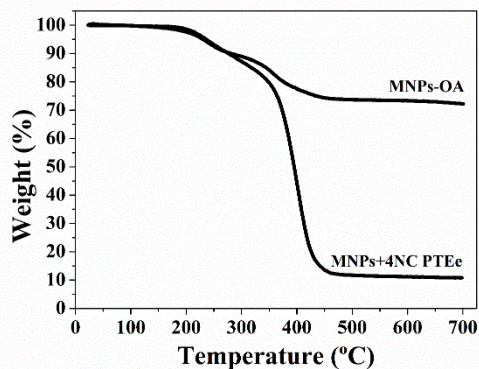
Source: From the author.

Figure 22 illustrates the magnetization curves of MNPs-OA and MNPs+4NC PTEe nanoparticles at room temperature, which were obtained by VSM analyses. Both samples showed typical superparamagnetic behavior, as shown by the absence of coercivity and remanence magnetization, and high saturation magnetization (FEUSER et al., 2014; SOARES et al., 2016). In this way, without an external magnetic field, their overall magnetization value is randomized to zero, avoiding interactive behavior of the particles when there is no applied field (MODY et al., 2014). Again, the MNPs-PTEe have similar behavior compared to the 4NC+MNPs PTEe, so its magnetization curve is not displayed in the graph. The superparamagnetic proprieties are very important for the application of the material in the biomedical field. Thus, this result indicates that the superparamagnetic properties of the MNPs+4NC PTEe nanoparticles are favorable for their use in biomedical applications (MODY et al., 2014).

Figure 22. VSM analyses of MNPs coated with OA and MNPs+4NC PTEe nanoparticles.
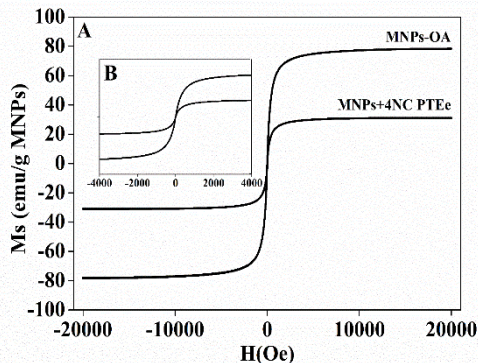
Source: From the author.

4.3.2   *In vitro* 4NC release profile

An *in vitro* release study was performed in order to evaluate the release profile of 4NC loaded poly(thioether-ester) nanoparticles. The amount of 4NC released from the PTEe NPs reached 28% after the first 24 h and 70% after 17 days for the medium with pH 7.4. The release profile when nanoparticles were dispersed in a pH 6.0 medium were considerably faster. The amount of 4NC released in the medium reached 53% in 24 h and 89% after 17 days. These results are displayed in Figure

23A and can indicate that the 4NC from the nanoparticles would be released faster in the tumor environment, as it was expected according to the literature (FEUSER et al., 2015b; THORAT et al., 2016, 2017). Such result can be advantageous considering that the nanoparticles will be magnetically guided to the tumor locus.

A little burst release was observed in the first hour, as shown in Figure 23B. Such phenomena may occur depending on the methods of synthesis and storage conditions of the samples. When the formulations are prepared via solvent evaporation, for example, an increase in the removal rate of the organic solvent causes an increase in the porosity of the polymer matrix, resulting in heterogeneous drug distributions (JALIL; NIXON, 1990; KISHIDA et al., 1998; MALLAPRAGADA; PEPPAS; COLOMBO, 1997). Diffusion and migration of the drug may also occur during the drying process as water moves to the surface and evaporates. Drugs can diffuse with water, resulting in an uneven distribution, with higher concentrations on the surface (HUANG; BRAZEL, 2001). It is important to mention that the dashed lines indicate only the profile's tendency, and do not represent any mathematical model applied on the experimental data.

The zero order, first order, Higuchi and Korsmeyer-Peppas mathematical models were evaluated and the choice of the best model was made by linear correlation (R^2), as it is displayed in Table 4. The zero order model was the one which best described the release of 4NC for the pH 7.4 medium (R^2 0.943). The pharmaceutical dosage forms following this profile, release the same amount of drug by unit of time. Thus, it is the ideal method of drug release when the objective is to achieve a pharmacological prolonged action (COSTA; LOBO, 2001). The Higuchi model presented the highest value of R^2 for the pH 6.0 medium, 0.894. This model is based on Fick's first law, whereby the release occurs by the diffusion of the drug within the delivery system (MATHEW; DEVI; KV, 2007; PAUL, 2011). Therefore, these results suggest that the release of 4NC from MNPs-PTEe nanoparticles synthesized via miniemulsification and solvent evaporation would be controlled by diffusion in the tumor environment.

Figure 23. Release profile of MNPs+4NC PTEe nanoparticles in pH 7.4 and pH 6.0 (A) and zoom of the first hour of release (B).
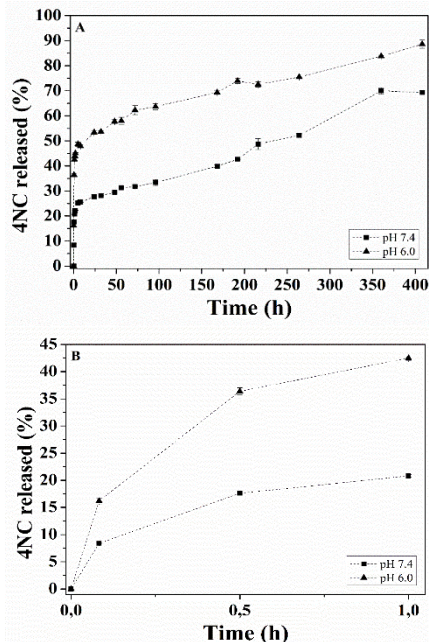
Source: From the author.

Table 4. Mathematical models used to evaluate the 4NC release profile and R^2 values for pH 7.4 and 6.0.

Mathematical models	Equation	R^2 pH 7.4	pH 6.0
Zero order	$Q_t = Q_0 + K_0 t$	0.943	0.768
First order	$lnQ_t = lnQ_0 + K_1 t$	0.738	0.514
Higuchi	$Q_t/Q_\infty = K_k t^n$	0.923	0.894
Korsmeyer-Peppas	$Q_t = K_H \sqrt{t}$	0.783	0.719

Source: From the author.

4.4 CONCLUSION

Magnetic nanoparticles and 4-nitrochalcone were efficiently encapsulated in poly(thioether-ester) nanoparticles by the miniemulsification and solvent evaporation method. The incorporation of

4NC did not affect the material properties and characteristics. Thus, MNPs+4NC PTEe nanoparticles presented spherical morphology, an average diameter around 150 nm, narrow average size distribution, and superparamagnetic properties. The nanoparticles exhibit an 4NC average encapsulation efficiency of up to 96 %. Furthermore, the release profile was evaluated and it was found that 4NC release occurred trough diffusion and faster in a medium with pH similar to tumor cells environment. Hence, these results corroborate the ones from the previous chapter, since an anticancer agent was successfully encapsulated and its release profile was obtained both for the physiological and the tumor environments.

CHAPTER V

5 ENCAPSULATION OF MAGNETIC NANOPARTICLES VIA MINIEMULSION POLYMERIZATION

5.1 INTRODUCTION

Polymeric nanoparticles (NPs) have been considered as an effective system for the treatment of certain diseases since they contribute to a precise drug delivery at the desired region of the body (KONERACKÁ et al., 2008). Besides avoiding the use of organic solvents, the major advantage of using the method of miniemulsion polymerization to produce NPs is the possibility of incorporate inorganic nanoparticles – such as MNPs – in a single reaction stage and with high polymerization rates (LANDFESTER; MAILÄNDER, 2013; MAHDAVIAN; ASHJARI; MOBARAKEH, 2008; QIU et al., 2007). In miniemulsion polymerization, the first stage consists in the formation of small droplets of 50 to 500 nm by the dispersion of a system containing the dispersed phase and the continuous phase through a high shear apparatus, for example an ultrasound probe. In the second step, these droplets are polymerized by addition of initiator and increase in temperature (LANDFESTER, 2006). Thus, the polymeric nanoparticles formed by this method will have the function of protecting and preventing the aggregation of MNPs (TANG; HASHMI; SHAPIRO, 2013), while the MNPs will be able to guarantee the mobility of the NPs when a magnetic field is applied (ANGELOPOULOU et al., 2017; GULIN-SARFRAZ et al., 2014; NOWICKA et al., 2013; PRIJIC et al., 2010; QIU et al., 2017).

The thiol-ene polymerization in miniemulsion is a new field of study. Only after 2014, articles describing the synthesis of linear polymers by thiol-ene polymerization have been published (AMATO et al., 2015; CARDOSO et al., 2017; JASINSKI et al., 2014). Its unique attributes – including mild conditions, rapid reaction rates and without the formation of byproducts – can be inspiring for researching in polymer chemistry areas, such as applications in the biomedical field (CARDOSO et al., 2017).

Few studies have been already developed regarding the encapsulation of MNPs via miniemulsion polymerization (CHIARADIA et al., 2015; FEUSER et al., 2015a, 2015b; JIN et al., 2018; MAHDIEH; MAHDAVIAN; SALEHI-MOBARAKEH, 2017). Hence, the objective

of the work presented in this chapter was the encapsulation and characterization of MNPs in PTEe via thiol-ene miniemulsion polymerization as well as the characterization of the materials.

5.2 MATERIALS AND METHODS

5.2.1 Materials

The synthesis of the MNPs involved the following reagents: ferrous sulfate (FeSO$_4$·4H$_2$O), iron (III) chloride hexahydrate (FeCl$_3$·6H$_2$O), ammonium hydroxide (99%) and oleic acid (OA), all purchased from Vetec. The renewable monomer and the encapsulation of MNPs in PTEe were made with 10-undecenoic acid (Sigma-Aldrich, 98%), 1,3-propanediol (Sigma-Aldrich, 99.6%), p-toluenesulfonic acid monohydrate (Sigma-Aldrich, 98.5%), sodium dodecyl sulfate (SDS, Vetec), azobisisobutyronitrile (AIBN, Vetec, 98%), potassium persulfate (KPS, Vetec, 99%), 1,4-buthanedithiol (Sigma-Aldrich, >97%) and pentaerythritol tetrakis(3-mercaptopropionate) (PETMP, Sigma-Aldrich, > 95%). Distilled water was used throughout the experiments.

5.2.2 Synthesis of superparamagnetic poly(thioether-ester) nanoparticles via miniemulsion polymerization

The synthesis of the MNPs-OA was made as described in Chapter 3, session 3.2.3.

MNPs-PTEe nanoparticles were prepared by thiol-ene polymerization in miniemulsion. The aqueous phase was prepared with distilled water and 0.019 wt. % of SDS as surfactant. This phase was magnetically stirred until complete surfactant solubilization.

The organic phase was divided in two. The first one containing only 0.29 mL (2.45 mmol) of 1,4-butanedithiol (BDT). And the second containing 1 g (2.45 mmol) of 1,3-propylene diundec-10-enoate (Pd10e), 1 mol % (relative to BDT) of organic-soluble initiator (AIBN) and MNPs coated with oleic acid (MNPs-OA) at different concentrations (5, 10 and 35%) in relation to monomers combined weight. Organic phase 2, which contained MNPs-OA, was sonicated (Fisher Scientific Sonic Dismembrator model 500 and a 1/2" tip) for 1 min (10 s on and 5 s off) in ice bath at 30% of amplitude, to ensure the dispersion of MNPs-OA in Pd10e.

Next, half of the aqueous phase was added to the organic phase containing only BDT. The mixture was let under magnetic stirring to form a macro-emulsion. The other half of the aqueous phase was added to the second organic phase and placed in the ultrasound probe for 1 min (10 s on and 5 s off) in ice bath at 30% of amplitude, to form a macro-emulsion. Subsequently both macro-emulsions underwent sonication separately (2 min, 10 s on and 5 s off, at 70 % of amplitude in ice bath) to form miniemulsions. Finally, these miniemulsions were mixed and once again sonicated under same conditions. The final miniemulsion underwent polymerization at 80 °C for 4 h in a thermostatic bath.

A multifunctional thiol, pentaerythritol tetrakis(3-mercaptopropionate) (PETMP), was also applied in order to obtain cross-linked PTEe and increase the incorporation of MNPs. In this case, BDT was totally replaced by PETMP, 2 mL of chloroform was added to the organic phase and KPS was used as initiator and added to the final miniemulsion due to coagulation caused by premature polymerization. This method is illustrated in Figure 24.

Figure 24. Scheme of the encapsulation of MNPs via miniemulsion polymerization.
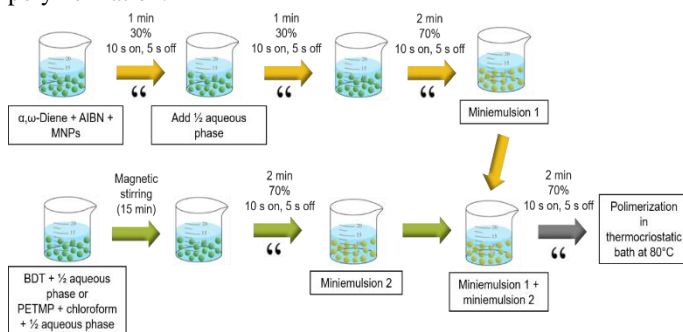
Source: From the author.

5.2.3 Characterization

Particle size, polydispersity index, surface charge, thermogravimetric analysis, chemical characterization, hysteresis loops measurements, and morphology characterization of the nanoparticles were performed following the procedure described in Chapter 3, session 3.3.5.

5.3 RESULTS AND DISCUSSION

5.3.1 Synthesis of superparamagnetic poly(thioether-ester) via miniemulsion polymerization

5.3.1.1   Nanoparticles characterization

Table 5 shows the mean diameter (Dp), polydispersity index (PdI) and zeta potential obtained by DLS. Samples exhibited good particle diameters, however some polydispersity indexes were a little bit higher than expected. Also, these values were higher when compared to the samples synthesized by miniemulsification and solvent evaporation. However, the nanoparticles still presented diameters which, according to the literature, could maximize the cellular uptake and avoid sequestration and extravasation to the tissues (MOGHIMI; HUNTER; MURRAY, 2001). The zeta potential values obtained were lower than −40 mV at physiological pH, indicating good stability without formation of aggregates, which contributes to a higher colloidal stability (JASINSKI et al., 2016; MOGHIMI; HUNTER; MURRAY, 2001).

Table 5. Intensity mean diameters (Dp); polydispersity indexes (PdI) and zeta potentials in pH 7.

Sample	Thiol	MNPs (%)	Dp (nm)	PdI	Zeta Potential (mV)
blank PTEe	BDT	-	143 ± 4	0.20 ± 0.03	-42 ± 3
1	BDT	5	136 ± 4	0.42 ± 0.02	-46 ± 1
2	BDT	10	145 ± 11	0.42 ± 0.10	-47 ± 1
3	BDT	35	92 ± 12	0.25 ± 0.07	-47 ± 2
4	PETMP	5	165 ± 4	0.19 ± 0.02	-42 ± 2
5	PETMP	10	141 ± 16	0.13 ± 0.03	-42 ± 1
6	PETMP	35	259 ± 75	0.34 ± 0.10	-48 ± 0

$\pm$ Mean Standard deviation of n = 3 determinations
Source: From the author.

A TEM image of sample 5 is displayed in Figure 25. It can be seen that these nanoparticles presented spherical morphology and diameters around 100 nm, corroborating with the DLS analyses. It is also possible to see the MNPs incorporated, which are attributed to the darker points inside de nanoparticles in the figure. Comparing to the samples

synthesized by miniemulsification and solvent evaporation, the MNPs are more heterogeneously dispersed.

Figure 25. TEM image of sample 5 (PETMP – 10 % of MNPs).
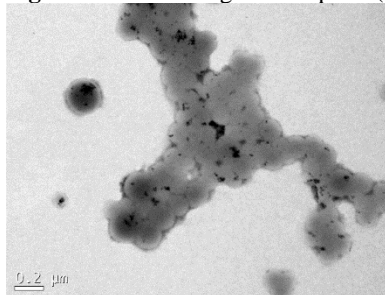
Source: From the author.

Thermogravimetry analyses were performed to evaluate the thermal decomposition of MNPs+PTEe as well as the amount of MNPs incorporated in the formulations. Table 6 presents the encapsulation efficiencies for all of the samples, which vary in type of thiol used, and in percentage of MNPs. The value of 35 % was chosen to compare the *in situ* method with the miniemulsification and solvent evaporation method. It is possible to notice that the efficiency of MNPs incorporation (EE%) decreased with the increase of MNPs (%) added to the formulation. Also, formulations in which PETMP was used were able to incorporate a higher amount of MNPs.

Table 6. Encapsulation efficiency (%) of MNPs obtained by TGA for samples 1 to 6.

Sample	Thiol	MNPs-OA (%)[a]	MNPs (%)[b]	Residue (%)	EE (%)
1	BDT	5	3.3	2.1	64.2
2	BDT	10	6.1	1.6	26.4
3	BDT	35	18.9	1.3	6.9
4	PETMP	5	3.2	3.1	95.8
5	PETMP	10	6.2	4.3	69.4
6	PETMP	35	19.1	7.2	37.7

[a] Theoretical percentage of MNPs-OA contained in the formulation. [b] Percentage of MNPs considering a concentration of 28 % of OA
Source: From the author.

        Sample 1, prepared with BDT and 5 % of MNPs, and sample 4, prepared with PETMP and 5 % of MNPs were chosen for the following characterization analyses due to their high encapsulation efficiency.

        The thermal decompositions of samples 1 (BDT) and 4 (PETMP) are displayed in Figure 26. The results had a similar behavior compared to the MNPs-PTEe synthesized by the miniemulsification and solvent evaporation method.

Figure 26. TGA analyses of MNPs-OA and samples 1 (BDT – 5 % of MNPs) and 4 (PETMP – 5 % of MNPs).
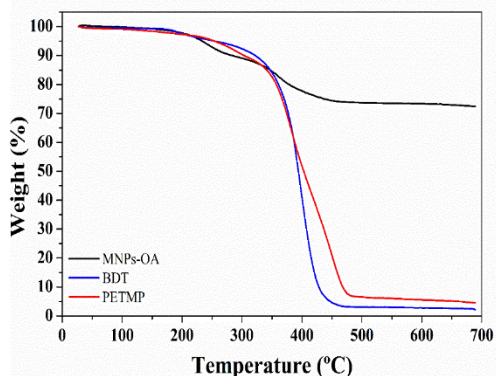
Source: From the author.

Figure 27. FTIR analyses of the samples 1 (BDT – 5 % of MNPs) and 4 (PETMP – 5 % of MNPs), blank PTEe and MNPs-OA.
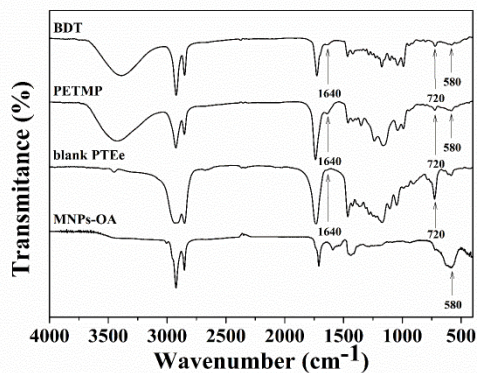
Source: From the author.

Figure 28 illustrates the magnetization curves obtained by VSM of samples 1 and 2, prepared with BDT, and samples 4 and 5, with PETMP, at room temperature. Both samples showed typical superparamagnetic behavior, as shown by the absence of coercivity and remanence magnetization, and high saturation magnetization (FEUSER et al., 2014; SOARES et al., 2016). MNPs-PTEe synthesized by miniemulsion polymerization showed similar behavior compared to the MNPs-PTEe obtained by miniemulsification and solvent evaporation. Differences in the Ms value occurred due to the differences in the amounts of MNPs incorporated in each sample. Thus, as expected, the Ms values are higher for the samples with higher amount of MNPs incorporated.

Figure 28. VSM analyses of samples 1 (BDT – 5 % of MNPs) and 4 (PETMP – 5 % of MNPs).
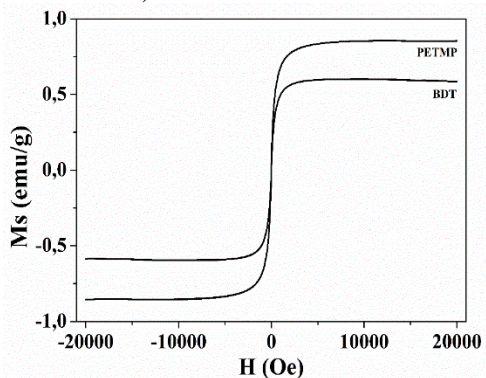
Source: From the author.

5.4 CONCLUSION

Magnetic nanoparticles were incorporated in poly(thioether-ester) with an increase of Dp and PdI values comparing to the samples synthesized by miniemulsification and solvent evaporation. However, nanoparticles presented spherical morphology and Dp values still are in the ideal range to be applied in biomedical purposes. Quantitatively, it was possible to observe that the percentage of incorporation of MNPs increased with the decrease of the amount of MNPs added to the formulation. Also, formulations with PETMP presented higher efficiencies. Finally, the material presented superparamagnetic behavior, which is extremely important for biomedical applications. Thus, it was

possible to produce MNPs-PTEe through a more efficient and environmentally friendly method. Through miniemulsion polymerization it was possible to obtain encapsulation efficiencies of MNPs as high as through miniemulsification and solvent evaporation method. Also, this method presents the advantage of incorporating such material in only one step and without using organic solvents

CHAPTER VI

6   CONCLUSION

Superparamagnetic nanoparticles and the anticancer agent 4-nitrochalcone (4NC) were successfully encapsulated in PTEe using two different methods and were characterized. Through miniemulsification and solvent evaporation, the nanoparticles presented spherical morphology, Dp between 120 and 150 nm and low PdI. FT-IR analyses showed the absorption bands of both the polymer and the MNPs. TGA analyses showed an EE% of MNPs greater than 99%. VSM analyses showed that the materials have superparamagnetic characteristics. Cytotoxicity assay in HeLa cells has demonstrated that the material is not cytotoxic. Fluorescence microscopy assay, also in HeLa cells, demonstrated that when exposed to an external magnetic field, the cell uptake is up to three times higher. The EE% of 4NC was greater than 90%. The release profile of 4NC was obtained at pH 7.4 and 6.0, using a sample of MNPs and 4NC simultaneously encapsulated. It was observed that the release occurs by diffusion and more rapidly at pH 6.0.

Using miniemulsion polymerization, the nanoparticles also presented spherical morphology, but Dp and PdI were slightly higher. The MNPs were encapsulated at different concentrations and, through TGA, it was observed that the higher the initial percentage of MNPs, the lower their EE%. In addition, it can be seen that using a tetrathiol in the formulation, rather than a dithiol, the EE% of MNPs was greater. This method presents the advantage of being able to incorporate MNPs in only one step. Although more assays are necessary to prove its effectiveness, the synthesized materials demonstrated potential to be used in biomedical applications such as cancer treatment.

6.1 FURTHER WORKS

- Simultaneous encapsulation of MNPs and 4NC via miniemulsion polymerization;
- In vivo toxicity studies;
- Hyperthermia assays in HeLa cells;
- Deeper studies of the 4NC release profiles.

REFERENCES

AMATO, D. V. et al. Functional, sub-100 nm polymer nanoparticles via thiol-ene miniemulsion photopolymerization. **Polymer Chemistry**, [s. l.], v. 6, n. 31, p. 5625–5632, 2015.

AMBROGIO, Michael W. et al. Mechanized Silica Nanoparticles: A New Frontier in Theranostic Nanomedicine. [s. l.], v. 44, n. 10, p. 903–913, 2011.

AMERICAN CANCER SOCIETY. Cancer Facts & Figures 2015. **Cancer Facts & Figures 2015**, [s. l.], p. 1–9, 2015.

ANGELOPOULOU, Athina et al. Magnetic Nanoparticles for the Delivery of Dapagliflozin to Hypoxic Tumors: Physicochemical Characterization and Cell Studies. **AAPS PharmSciTech**, [s. l.], 2017.

ANTONIETTI, Markus; LANDFESTER, Katharina. Polyreactions in miniemulsions. **Progress in Polymer Science (Oxford)**, [s. l.], v. 27, n. 4, p. 689–757, 2002.

ARSHADY, R. Microcapsules for food. **Journal of Microencapsulation**, [s. l.], v. 10, n. 4, p. 413–435, 1993.

ASUA, José M. Miniemulsion polymerization. **Progress in Polymer Science**, [s. l.], v. 27, n. 7, p. 1283–1346, 2002. Disponível em: <http://linkinghub.elsevier.com/retrieve/pii/S0079670002000102>

ASUA, José M. Mapping the morphology of polymer-inorganic nanocomposites synthesized by miniemulsion polymerization. **Macromolecular Chemistry and Physics**, [s. l.], v. 215, n. 5, p. 458–464, 2014.

BAKER, R. **Controlled release of biologically active agents**. New York: John Wiley & Sons, p.206-214,1986.

BHAT, B. A. et al. Synthesis and biological evaluation of chalcones and their derived pyrazoles as potential cytotoxic agents. **Bioorganic and Medicinal Chemistry Letters**, [s. l.], v. 15, n. 12, p. 3177–3180, 2005.

BLANCO, Elvin et al. Nanomedicine in cancer therapy: Innovative trends and prospects. **Cancer Science**, [s. l.], v. 102, n. 7, p. 1247–1252, 2011.

BRAZEL, C.S.; PEPPAS, N.A. Temperature- and pH-sensitive hydrogels for controlled release of antithrombotic agents, Mater. Res. Soc. Symp. Proc. 331 (1994) 211–216.

CARDOSO, Priscilla B. et al. Biocompatible polymeric nanoparticles from castor oil derivatives via thiol-ene miniemulsion polymerization. **European Journal of Lipid Science and Technology**, [s. l.], v. 120, p. 1700212, 2017.

CHIARADIA, Viviane et al. Incorporation of superparamagnetic nanoparticles into poly(urea-urethane) nanoparticles by step growth interfacial polymerization in miniemulsion. **Colloids and Surfaces A: Physicochemical and Engineering Aspects**, [s. l.], v. 482, p. 596–603, 2015.

COSTA, Paulo; LOBO, Jose Manuel Sousa. Modeling and comparison of dissolution profile. **European Journal of Pharmaceutical Sciences**, [s. l.], v. 13, p. 123–133, 2001.

COWAN, Marjorie Murphy. Plant Products as Antimicrobial Agents. **Clinical Microbial Reviews**, [s. l.], v. 12, n. 4, p. 564–582, 1999.

CRAMER, Neil B.; BOWMAN, Christopher N. Kinetics of thiol-ene and thiol-acrylate photopolymerizations with real-time Fourier transform infrared. **Journal of Polymer Science, Part A: Polymer Chemistry**, [s. l.], v. 39, n. 19, p. 3311–3319, 2001.

CRESPY, Daniel; LANDFESTER, Katharina. Miniemulsion polymerization as a versatile tool for the synthesis of functionalized polymers. **Beilstein Journal of Organic Chemistry**, [s. l.], v. 6, p. 1132–1148, 2010.

CULLITY, B.D. Introduction to Magnetic Materials. Addison-Wesley, Reading, 1972.
DALLA VIA, Lisa et al. DNA-targeting pyrroloquinoline-linked

butenone and chalcones: Synthesis and biological evaluation. **European Journal of Medicinal Chemistry**, [s. l.], v. 44, n. 7, p. 2854–2861, 2009.

DANHIER, Fabienne; FERON, Olivier; PRÉAT, Véronique. To exploit the tumor microenvironment: Passive and active tumor targeting of nanocarriers for anti-cancer drug delivery. **Journal of Controlled Release**, [s. l.], v. 148, n. 2, p. 135–146, 2010. Disponível em: <http://dx.doi.org/10.1016/j.jconrel.2010.08.027>

DAVE, Shivang R.; GAO, Xiaohu. Monodisperse magnetic nanoparticles for biodetection, imaging, and drug delivery: a versatile and evolving technology. **Nanomedicine and Nanobiotechonology**, [s. l.], v. 1, p. 583–609, 2009.

DETSI, Anastasia et al. Natural and synthetic 2′-hydroxy-chalcones and aurones: Synthesis, characterization and evaluation of the antioxidant and soybean lipoxygenase inhibitory activity. **Bioorganic and Medicinal Chemistry**, [s. l.], v. 17, n. 23, p. 8073–8085, 2009.

DIMMOCK, Jonathan R. et al. Correlations between cytotoxicity and topography of some 2-arylidenebenzocycloalkanones determined by X-ray crystallography. **Journal of Medicinal Chemistry**, [s. l.], v. 45, n. 14, p. 3103–3111, 2002.

DURÁN, N.; MATTOSO, L. H. C.; MORAIS, P. C. Nanotecnologia: Introdução, preparação e caracterização de nanomateriais e exemplos de aplicações. São Paulo, Artiliber, 2006; p.175-183.

ESCOBAR, STEPHANE JANAINA de MOURA. **EFEITOS DAS CHALCONAS SOBRE PROPRIEDADES OXIDATIVAS DE MITOCÔNDRIAS ISOLADAS DE FÍGADO DE RATO**. 2014. UNIVERSIDADE FEDERAL DO PARANÁ, [s. l.], 2014.

FELICE, Betiana et al. Drug delivery vehicles on a nano-engineering perspective. **Materials Science and Engineering C**, [s. l.], v. 41, p. 178–195, 2014.

FERLAY, Jacques et al. Cancer incidence and mortality worldwide: Sources, methods and major patterns in GLOBOCAN 2012. **International Journal of Cancer**, [s. l.], v. 136, n. 5, p. E359–E386, 2015.

FEUSER, Paulo E. et al. Synthesis and characterization of poly(methyl methacrylate) pmma and evaluation of cytotoxicity for biomedical application. **Macromolecular Symposia**, [s. l.], v. 343, n. 1, p. 65–69, 2014.

FEUSER, Paulo Emilio et al. Encapsulation of magnetic nanoparticles in poly(methyl methacrylate) by miniemulsion and evaluation of hyperthermia in U87MG cells. **European Polymer Journal**, [s. l.], v. 68, p. 355–365, 2015. a.

FEUSER, Paulo Emilio et al. Simultaneous encapsulation of magnetic nanoparticles and zinc phthalocyanine in poly(methyl methacrylate) nanoparticles by miniemulsion polymerization and in vitro studies. **Colloids and Surfaces B: Biointerfaces**, [s. l.], v. 135, p. 357–364, 2015. b.

FIORE, Cristina et al. A history of the therapeutic use of liquorice in Europe. **Journal of Ethnopharmacology**, [s. l.], v. 99, n. 3, p. 317–324, 2005.

FUKUMURA, Dai; JAIN, Rakesh K. Imaging angiogenesis and the microenvironment. **Cancer Treatment Reviews**, [s. l.], v. 116, n. 7–8, p. 695–715, 2008.

GIBBS, B. F. et al. Encapsulation in the food industry: a review. **International journal of food sciences and nutrition**, [s. l.], v. 50, n. 3, p. 213–224, 1999.

GRADY, K. O. Biomedical Applications of Magnetic Nanoparticles. **Journal of Physics D: Applied Physics**, [s. l.], v. 36, 2002.

GRIFFITH, L. G. Polymeric biomaterials. **Acta Materialia**, [s. l.], v. 48, p. 263–277, 2000.

GULIN-SARFRAZ, Tina et al. FRET-reporter nanoparticles to monitor redox-induced intracellular delivery of active compounds. **RSC Adv.**, [s. l.], v. 4, n. 32, p. 16429–16437, 2014.

GUPTA, Ajay Kumar; GUPTA, Mona. Synthesis and surface engineering of iron oxide nanoparticles for biomedical applications. **Biomaterials**, [s. l.], v. 26, n. 18, p. 3995–4021, 2005.

GUPTA, Ajay Kumar; WELLS, Stephen. Surface-Modified Superparamagnetic Nanoparticles for Drug Delivery: Preparation, Characterization, and Cytotoxicity Studies. **IEEE Transactions on Nanobioscience**, [s. l.], v. 3, n. 1, p. 66–73, 2004.

HARUSH-FRENKEL, Oshrat et al. Surface charge of nanoparticles determines their endocytic and transcytotic pathway in polarized MDCK cells. **Biomacromolecules**, [s. l.], v. 9, n. 2, p. 435–443, 2008.

HE, Chunbai et al. Effects of particle size and surface charge on cellular uptake and biodistribution of polymeric nanoparticles. **Biomaterials**, [s. l.], v. 31, n. 13, p. 3657–3666, 2010.

HE, Lei et al. Preparation of SiO2/(PMMA/Fe3O4) from monolayer linolenic acid modified Fe3O4 nanoparticles via miniemulsion polymerization. **Journal of Biomedical Nanotechnology**, [s. l.], v. 5, n. 5, p. 596–601, 2009.

HIGUCHI, W. I.; MISRA, Jagdish. Physical Degradation of Emulsions Via the Molecular Diffusion Route and the Possible Prevention Thereof. **Journal of Pharmaceutical Sciences**, [s. l.], v. 51, n. 5, p. 459–466, 1962.

HRIBAR, Kolin C. et al. Enhanced release of small molecules from near-infrared light responsive polymer-nanorod composites. **ACS Nano**, [s. l.], v. 5, n. 4, p. 2948–2956, 2011.

HSU, Li Ling et al. Chalcone inhibits the proliferation of human breast cancer cell by blocking cell cycle progression and inducing apoptosis. **International Journal of Mobile Communications**, [s. l.], v. 4, n. 6, p. 704–726, 2006.

HUANG, Xiao; BRAZEL, Christopher S. On the importance and mechanisms of burst release in matrix-controlled drug delivery systems. **Journal of Controlled Release**, [s. l.], v. 73, n. 2–3, p. 121–136, 2001.

ILANGO, Kaliappan; VALENTINA, Parthiban; SALUJA, Gurdeep Singh. Synthesis and In-vitro anti-cancer activity of some substituted chalcone derivatives. **Research Journal of Pharmaceutical, Biological and Chemical Sciences**, [s. l.], v. 1, n. 2, p. 354–359, 2010.

INSTITUTO NACIONAL DO CâNCER JOSÉ DE ALENCAR GOMES DA SILVA (INCA). **Estimate/2018 - Cancer Incidence in Brazil**. Rio de Janeiro.

INSTITUTO NACIONAL DO CâNCER JOSÉ DE ALENCAR GOMES DA SILVA (INCA). **O que é o câncer?** 2018. Disponível em: <http://www1.inca.gov.br/conteudo_view.asp?id=322>. Acesso em: 21 jun. 2018.

JABR-MILANE, Lara S. et al. MULTI-FUNCTIONAL NANOCARRIERS TO OVERCOME TUMOR DRUG RESISTANCE. **Cancer Treatment Reviews**, [s. l.], v. 34, n. 7, p. 592–602, 2008.

JALIL, R.; NIXON, J. R. Biodegradable poly(1actic acid) and poly(1actide-co-glycolide) microcapsules: problems associated with preparative techniques and release properties. **Journal of Microencapsulation**, [s. l.], v. 7, n. 3, p. 297–325, 1990.

JASINSKI, Florent et al. Light-mediated thiol-ene polymerization in miniemulsion: A fast route to semicrystalline polysul fide nanoparticles. **ACS Macro Letters**, [s. l.], v. 3, n. 9, p. 958–962, 2014.

JASINSKI, Florent et al. Thiol-Ene Linear Step-Growth Photopolymerization in Miniemulsion: Fast Rates, Redox-Responsive Particles, and Semicrystalline Films. **Macromolecules**, [s. l.], v. 49, n. 4, p. 1143–1153, 2016.

JEONG, Byeongmoon; BAE, You Han; KIM, Sung Wan. Drug release from biodegradable injectable thermosensitive hydrogel of PEG – PLGA – PEG triblock copolymers. **Journal of Controlled Release**, [s. l.], v. 63, p. 155–163, 2000.

JIN, Xin et al. In vitro and in vivo evaluation of 10-hydroxycamptothecin-loaded poly (n-butyl cyanoacrylate) nanoparticles prepared by miniemulsion polymerization. **Colloids and Surfaces B: Biointerfaces**, [s. l.], v. 162, p. 25–34, 2018.

JONG, W. H. De; BORM, P. J. A. Drug delivery and nanoparticles: applications and hazzards. **International Journal of Nanomedicine**, [s. l.], v. 3, n. 2, p. 133–149, 2008.

KISHIDA, Akio et al. Polymer Drugs and Polymeric Drugs X: Slow Release of 5-Fluorouracil from Biodegradable Poly(y-glutamic acid) and Its Benzyl Ester Matrices. **Journal of Bioactive and Compatible Polymers**, [s. l.], v. 13, p. 270–278, 1998.

KNOBEL, Marcelo. Partículas Finas: Superparamagnetismo e Magnetoresistência Gigante. **Revista Brasileira de Ensino de Física**, [s. l.], v. 22, n. 3, p. 387–395, 2000.

KONERACKÁ, M. et al. Encapsulation of anticancer drug and magnetic particles in biodegradable polymer nanospheres. **Journal of physics. Condensed matter : an Institute of Physics journal**, [s. l.], v. 20, n. 20, p. 204151, 2008.

KONG, Seong Deok et al. Acidic hydrolysis of N-ethoxybenzylimidazoles (NEBIs): Potential applications as pH-sensitive linkers for drug delivery. **Bioconjugate Chemistry**, [s. l.], v. 18, n. 2, p. 293–296, 2007.

LANDFESTER, K. Synthesis of Colloidal Particles in Miniemulsions. **Annual Review of Materials Research**, [s. l.], v. 36, n. 1, p. 231–279, 2006.

LANDFESTER, Katharina. Miniemulsion polymerization and the structure of polymer and hybrid nanoparticles. **Angewandte Chemie - International Edition**, [s. l.], v. 48, n. 25, p. 4488–4508, 2009.

LANDFESTER, Katharina; MAILÄNDER, Volker. **Nanocapsules with specific targeting and release properties using miniemulsion polymerization**. **Expert Opinion on Drug Delivery**, [s. l.], v. 10, n. 5, p. 593–609, 2013.

LANDFESTER, Katharina; RAM REZ, Liliana P. Encapsulated magnetite particles for biomedical application. **Journal of Physics: Condensed Matter**, [s. l.], v. 15, n. 15, p. S1345–S1361, 2003.

LEIMANN, Fernanda Vit??ria et al. Hydrolysis of poly(hydroxybutyrate-co-hydroxyvalerate) nanoparticles. **Journal of Applied Polymer Science**, [s. l.], v. 128, n. 5, p. 3093–3098, 2013.

LIU, Xuesong et al. Induction of apoptotic program in cell-free extracts: Requirement for dATP and cytochrome c. **Cell**, [s. l.], v. 86, n. 1, p. 147–157, 1996.

M. VAN HERK, Alex; LANDFESTER, Katharina. **Hybrid Latex Particles Preparation with (Mini)emulsion Polymerization**. [s.l: s.n.].

MACDONALD, Cristin et al. Time-varied magnetic field enhances transport of magnetic nanoparticles in viscous gel. **Nanomedicine (London, England)**, [s. l.], v. 5, p. 65–76, 2010.

MACHADO, Thiago O.; SAYER, Claudia; ARAUJO, Pedro H. H. Thiol-ene polymerisation: A promising technique to obtain novel biomaterials. **European Polymer Journal**, [s. l.], v. 86, p. 200–215, 2017.

MAHAPATRA, Debarshi K. ar; BHARTI, Sanjay K. umar; ASATI, Vivek. Anti-cancer chalcones: Structural and molecular target perspectives. **European journal of medicinal chemistry**, [s. l.], v. 98, p. 69–114, 2015.

MAHAPATRA, Debarshi Kar; ASATI, Vivek; BHARTI, Sanjay Kumar. Chalcones and their therapeutic targets for the management of diabetes: Structural and pharmacological perspectives. **European Journal of Medicinal Chemistry**, [s. l.], v. 92, p. 839–865, 2015.

MAHDAVIAN, Ali Reza; ASHJARI, Mohsen; MOBARAKEH, Hamid Salehi. Nanocomposite Particles with Core-Shell Morphology. I. Preparation and Characterization of Fe3O4-Poly(butyl acrylate-styrene) Particles via Miniemulsion Polymerization. **Journal of Applied Polymer Science**, [s. l.], v. 110, p. 1242–1249, 2008.

MAHDIEH, Athar; MAHDAVIAN, Ali Reza; SALEHI-MOBARAKEH, Hamid. Chemical modification of magnetite nanoparticles and preparation of acrylic-base magnetic nanocomposite particles via miniemulsion polymerization. [s. l.], v. 426, n. August 2016, p. 230–238, 2017.

MALLAKPOUR, S.; BEHRANVAND, V. Polymeric nanoparticles: Recent development in synthesis and application. **Express Polymer Letters**, [s. l.], v. 10, n. 11, p. 895–913, 2016.

MALLAPRAGADA, Surya K.; PEPPAS, Nikolaos A.; COLOMBO, Paolo. Crystal dissolution-controlled release systems. II. Metronidazole release from semicrystalline poly(vinyl alcohol) systems. **Journal of Biomedical Materials Research**, [s. l.], v. 36, n. 1, p. 125–130, 1997.

MATHEW, Sam T.; DEVI, S. Gayathri; KV, Sandhya. Formulation and evaluation of ketorolac tromethamine-loaded albumin microspheres for potential intramuscular administration. **AAPS PharmSciTech**, [s. l.], v. 8, n. 1, p. 14, 2007.

MATSUMURA, Y.; MAEDA, H. A new concept for macromolecular therapeutics in cnacer chemotherapy: mechanism of tumoritropic accumulatio of proteins and the antitumor agents Smancs. **Cancer research**, [s. l.], v. 46, n. 12 Pt 1, p. 6387–6392, 1986.

MEIER, Michael A. R.; METZGER, Jürgen O.; SCHUBERT, Ulrich S. Plant oil renewable resources as green alternatives in polymer science. **Chemical Society Reviews**, [s. l.], v. 36, n. 11, p. 1788–1802, 2007.

MODY, Vicky V. et al. Magnetic nanoparticle drug delivery systems for targeting tumor. **Applied Nanoscience**, [s. l.], v. 4, n. 4, p. 385–392, 2014.

MOGHIMI, S. M.; HUNTER, A. C.; MURRAY, J. C. Long-circulating and target-specific nanoparticles: theory to practice. **Pharmacological reviews**, [s. l.], v. 53, n. 2, p. 283–318, 2001.

MONTERO DE ESPINOSA, Lucas; MEIER, Michael A. R. Plant oils: The perfect renewable resource for polymer science?! **European Polymer Journal**, [s. l.], v. 47, n. 5, p. 837–852, 2011.

MUSYANOVYCH, Anna et al. Preparation of biodegradable polymer nanoparticles by miniemulsion technique and their cell interactions. **Macromolecular Bioscience**, [s. l.], v. 8, n. 2, p. 127–139, 2008.

NAVARINI, Andréia Lilian Formento et al. Hydroxychalcones induce apoptosis in B16-F10 melanoma cells via GSH and ATP depletion. **European Journal of Medicinal Chemistry**, [s. l.], v. 44, n. 4, p. 1630–1637, 2009.

NEDOVIC, Viktor et al. An overview of encapsulation technologies for food applications. **Procedia Food Science**, [s. l.], v. 1, p. 1806–1815, 2011.

NOWAKOWSKA, Zdzisława. A review of anti-infective and anti-inflammatory chalcones. **European Journal of Medicinal Chemistry**, [s. l.], v. 42, n. 2, p. 125–137, 2007.

NOWICKA, Anna M. et al. Progress in targeting tumor cells by using drug-magnetic nanoparticles conjugate. **Biomacromolecules**, [s. l.], v. 14, n. 3, p. 828–833, 2013.

PALIWAL, Shivani Rai et al. Liposomal nanomedicine for breast cancer therapy R eview. [s. l.], v. 6, p. 1085–1100, 2011.

PARK, Tae Gwan; COHEN, Smadar; LANGER, Robert. **Controlled Protein Release from Polyethyleneimine-Coated Poly(L-lactic Acid)/Pluronic Blend MatricesPharmaceutical Research: An Official Journal of the American Association of Pharmaceutical Scientists**, 1992. a.

PARK, Tae Gwan; COHEN, Smadar; LANGER, Robert. Poly(l-lactic acid)/Pluronic Blends: Characterization of Phase Separation Behavior, Degradation, and Morphology and Use as Protein-Releasing Matrices. **Macromolecules**, [s. l.], v. 25, n. 1, p. 116–122, 1992. b.

PATIL, P. S. et al. Synthesis, growth, and characterization of 4-OCH3-4′-nitrochalcone single crystal: A potential NLO material. **Journal of Crystal Growth**, [s. l.], v. 297, n. 1, p. 111–116, 2006.

PATIL, R. M. et al. Non-aqueous to aqueous phase transfer of oleic acid coated iron oxide nanoparticles for hyperthermia application. **RSC Adv.**, [s. l.], v. 4, n. 9, p. 4515–4522, 2014.

PAUL, D. R. Elaborations on the Higuchi model for drug delivery. **International Journal of Pharmaceutics**, [s. l.], v. 418, n. 1, p. 13–17, 2011.

PICH, Andrij et al. Preparation of poly(3-hydroxybutyrate-co-3-hydroxyvalerate) (PHBV) particles in O/W emulsion. **Polymer**, [s. l.], v. 47, n. 6, p. 1912–1920, 2006.

PINTO REIS, Catarina et al. Nanoencapsulation I. Methods for preparation of drug-loaded polymeric nanoparticles. **Nanomedicine: Nanotechnology, Biology, and Medicine**, [s. l.], v. 2, n. 1, p. 8–21, 2006.

POLETTO, Fernanda S. et al. Controlling the size of poly(hydroxybutyrate-co-hydroxyvalerate) nanoparticles prepared by emulsification-diffusion technique using ethanol as surface agent. **Colloids and Surfaces A: Physicochemical and Engineering Aspects**, [s. l.], v. 324, n. 1–3, p. 105–112, 2008.

PRABHAKAR, Uma et al. Challenges and key considerations of the enhanced permeability and retention effect for nanomedicine drug delivery in oncology. **Cancer Research**, [s. l.], v. 73, n. 8, p. 2412–2417, 2013.

PRAKASH, Om et al. Anticancer Potential of Plants and Natural Products: A Review. **American Journal of Pharmacological Sciences**, [s. l.], v. 1, n. 6, p. 104–115, 2013.

PRIJIC, Sara et al. Increased cellular uptake of biocompatible superparamagnetic iron oxide nanoparticles into malignant cells by an external magnetic field. **Journal of Membrane Biology**, [s. l.], v. 236, n. 1, p. 167–179, 2010.

QIU, Guihua et al. Polystyrene/Fe3O4magnetic emulsion and nanocomposite prepared by ultrasonically initiated miniemulsion polymerization. **Ultrasonics Sonochemistry**, [s. l.], v. 14, n. 1, p. 55–61, 2007.

QIU, Yongzhi et al. Magnetic forces enable controlled drug delivery by disrupting endothelial cell-cell junctions. **Nature Communications**, [s. l.], v. 8, p. 1–10, 2017.

RAMACHANDRA RAO, S.; RAVISHANKAR, G. A. Plant cell cultures: Chemical factories of secondary metabolites. **Biotechnology Advances**, [s. l.], v. 20, n. 2, p. 101–153, 2002.

RÉ, Maria I. Microencapsulation by spray drying. **Drying Technology: An International Journal**, [s. l.], v. 16, n. 6, p. 1195–1236, 1998.

REN, Tianbin et al. Reduction-cleavable polymeric vesicles with efficient glutathione-mediated drug release behavior for reversing drug resistance. **ACS Applied Materials and Interfaces**, [s. l.], v. 5, n. 21, p. 10721–10730, 2013.

REZENDE, S. M. A física de materiais e dispositivos eletrônicos, Recife, ed. UFPE. p.530, 1996.

RIBEIRO, Guiliano Augustus Pavan. As Propriedades Magnéticas da Matéria: um primeiro contato. **Revista Brasileira do Ensino de Física**, [s. l.], v. 22, n. 3, p. 299–305, 2000.

RICCI-JÚNIOR, Eduardo; MARCHETTI, Juliana Maldonado. Zinc(II) phthalocyanine loaded PLGA nanoparticles for photodynamic therapy use. **International Journal of Pharmaceutics**, [s. l.], v. 310, n. 1–2, p. 187–195, 2006.

ROMIO, Ana Paula et al. Encapsulation of magnetic nickel nanoparticles via inverse miniemulsion polymerization. **Journal of Applied Polymer Science**, [s. l.], v. 129, n. 3, p. 1426–1433, 2013.

SAHOO, Banalata et al. Thermal and pH responsive polymer-tethered

multifunctional magnetic nanoparticles for targeted delivery of anticancer drug. **ACS Applied Materials and Interfaces**, [s. l.], v. 5, n. 9, p. 3884–3893, 2013.

SAIYED, Zainulabedin M.; GANDHI, Nimisha H.; NAIR, Madhavan P. N. Magnetic nanoformulation of azidothymidine 5'-triphosphate for targeted delivery across the blood-brain barrier. **International Journal of Nanomedicine**, [s. l.], v. 5, n. 1, p. 157–166, 2010.

SCHAFFAZICK, Scheila Rezende et al. Caracterização e estabilidade físico-química de sistemas poliméricos nanoparticulados para administração de fármacos. **Quimica Nova**, [s. l.], v. 26, n. 5, p. 726–737, 2003.

SHAHIDI, Fereidoon; AMBIGAIPALAN, Priyatharini. Phenolics and polyphenolics in foods, beverages and spices: Antioxidant activity and health effects - A review. **Journal of Functional Foods**, [s. l.], v. 18, p. 820–897, 2015.

SHETE, P. B. et al. Magnetic chitosan nanocomposite for hyperthermia therapy application: Preparation, characterization and in vitro experiments. **Applied Surface Science**, [s. l.], v. 288, p. 149–157, 2014.

SHIVELY, M. L. et al. Physico-chemical characterization of a polymeric injectable implant delivery system. **Journal of Controlled Release**, [s. l.], v. 33, n. 2, p. 237–243, 1995.

SIGMA-ALDRICH. **IR Spectrum Table & Chart**. 2018. SILVERSTAIN, Robert M.; WEBSTER, Francsis X.; KIEMLE, David J. **Spectrometric identification od organic compounds**. 7th. ed. [s.l.] : John Wiley & Sons, Inc., 2005.

SINNECKER, João Paulo. Materiais Magnéticos Doces e Materiais Ferromagnéticos Amorfos. **Revista Brasileira de Ensino de Física**, [s. l.], v. 22, n. 3, p. 396–405, 2000.

SKIBOLA, Christine F.; SMITH, Martyn T. Potential health impacts of excessive flavonoid intake. **Free Radical Biology & Medicine**, [s. l.], v. 29, n. 00, p. 375–383, 2000.
SOARES, Paula I. P. et al. Iron oxide nanoparticles stabilized with a

bilayer of oleic acid for magnetic hyperthermia and MRI applications. **Applied Surface Science**, [s. l.], v. 383, p. 240–247, 2016.

SOARES, Mariana V. et al. Improving the phototoxicity of the zinc phthalocyanine by encapsulation in nanoparticles: Preparation, characterization and phototherapy studies. **Latin American Journal of Pharmacy**, [s. l.], v. 29, n. 1, p. 5–12, 2010.

SRIVASTAVA, Y. K. Ecofriendly microwave assisted synthesis of some chalcones. **Rasayan Journal of Chemistry**, [s. l.], v. 1, n. 4, p. 884–886, 2008.

STAUDT, Thiago et al. Magnetic Polymer / Nickel Hybrid Nanoparticles Via Miniemulsion Polymerization. **Macromolecular Chemistry and Physics**, [s. l.], v. 214, p. 2213–2222, 2013.

STEWART, B. W.; WILD, C. P. World cancer report 2014. **World Health Organization**, [s. l.], p. 1–2, 2014.

STONER, E. C.; WOLHFARTH, E. P. **A mechanism of magnetic hysteresis in heterogeneous alloys**LondonThe Royal Society, , 1948.

TAKAHASHI, Tetsuyuki et al. Isoliquiritigenin, a flavonoid from licorice, reduces prostaglandin E2 and nitric oxide, causes apoptosis, and suppresses aberrant crypt foci development. **Cancer Science**, [s. l.], v. 95, n. 5, p. 448–453, 2004.

TAN, Aaron et al. Quantum dots and carbon nanotubes in oncology: A review on emerging theranostic applications in nanomedicine. **Nanomedicine**, [s. l.], v. 6, n. 6, p. 1101–1114, 2011.

TANG, Kevin S.; HASHMI, Sarah M.; SHAPIRO, Erik M. The effect of cryoprotection on the use of PLGA encapsulated iron oxide nanoparticles for magnetic cell labeling. **Nanotechnology**, [s. l.], v. 24, n. 12, p. 125101, 2013.

TARTAJ, Pedro et al. The preparation of magnetic nanoparticles for applications in biomedicine. **In Vivo**, [s. l.], v. 182, 2003.

TEJA, Amyn S.; KOH, Pei Yoong. Synthesis, properties, and

applications of magnetic iron oxide nanoparticles. **Progress in Crystal Growth and Characterization of Materials**, [s. l.], v. 55, n. 1–2, p. 22–45, 2009.

THORAT, Nanasaheb D. et al. Superparamagnetic iron oxide nanocargoes for combined cancer thermotherapy and MRI applications. **Physical Chemistry Chemical Physics**, [s. l.], v. 18, n. 31, p. 21331–21339, 2016.

THORAT, Nanasaheb D. et al. Effective Cancer Theranostics with Polymer Encapsulated Superparamagnetic Nanoparticles: Combined Effects of Magnetic Hyperthermia and Controlled Drug Release. **ACS Biomaterials Science and Engineering**, [s. l.], v. 3, n. 7, p. 1332–1340, 2017.

TRIERWEILER, Luciane Ferreira; TRIWERWEILER, Jorge O. Industrial Production of Polymeric Nanoparticles: Alternatives and Economic Analysis. In: Porto Alegre. p. 123–138.

UHRICH, K. E.; CANNIZZARO, S. M. Polymeric systems for controlled drug release. **Chemical Reviews**, [s. l.], v. 99, p. 3181−3198, 1999.

VEISEH, Omid et al. In vivo safety evaluation of polyarginine coated magnetic nanovectors. **Molecular Pharmaceutics**, [s. l.], v. 10, n. 11, p. 4099–4106, 2013.

WEBB, S. In the beginning. In: **The physics of medical imaging**. 2nd. ed. New York: Taylor & Francis, 2006. p. 7–19.

XIAO, Xiu ying et al. Licochalcone A inhibits growth of gastric cancer cells by arresting cell cycle progression and inducing apoptosis. **Cancer Letters**, [s. l.], v. 302, n. 1, p. 69–75, 2011.

XIAOLIN ZI AND ANNE R. SIMONEAU. Flavokawain A , a Novel

Chalcone from Kava Extract , Induces Apoptosis in Bladder Cancer Cells by Involvement of Bax Protein-Dependent and Mitochondria-Dependent Apoptotic Pathway and Suppresses Tumor Growth in Mice. **Cancer Res 2005;65:3479-3486.**, [s. l.], v. 65, n. 16, p. 3479–3486, 2005.

XIE, Songbo et al. Superparamagnetic iron oxide nanoparticles coated with different polymers and their MRI contrast effects in the mouse brains. **Applied Surface Science**, [s. l.], v. 326, p. 32–38, 2015.

YANG, Hong et al. Multifunctional core/shell nanoparticles cross-linked polyetherimide-folic acid as efficient notch-1 siRNA carrier for targeted killing of breast cancer. **Scientific Reports**, [s. l.], v. 4, p. 1–10, 2014.

YOON, G.; JUNG, Y. D.; CHEON, S. H. Cytotoxic allyl retrochalcone from the roots of Glycyrrhiza inflata. **Chem Pharm Bull (Tokyo)**, [s. l.], v. 53, n. 6, p. 694–695, 2005.

YOSHIMURA, Tsubasa et al. Bio-based polymer networks by thiol-ene photopolymerizations of allyl-etherified eugenol derivatives. **European Polymer Journal**, [s. l.], v. 67, p. 397–408, 2015.

ZÁVIŠOVÁ, Vlasta et al. Encapsulation of indomethacin in magnetic biodegradable polymer nanoparticles. **Journal of Magnetism and Magnetic Materials**, [s. l.], v. 311, n. 1 SPEC. ISS., p. 379–382, 2007.

ZHANG, Leyang et al. Camptothecin derivative-loaded poly(caprolactone-co-lactide)-b-PEG-b- poly(caprolactone-co-lactide) nanoparticles and their biodistribution in mice. **Journal of Controlled Release**, [s. l.], v. 96, n. 1, p. 135–148, 2004.

ZHAO, X. et al. Active scaffolds for on-demand drug and cell delivery. **Proceedings of the National Academy of Sciences**, [s. l.], v. 108, n. 1, p. 67–72, 2011.

ZHAO, Xueling et al. Multifunctional superparamagnetic Fe3O4@SiO

2 core/shell nanoparticles: Design and application for cell imaging. **Journal of Biomedical Nanotechnology**, [s. l.], v. 10, n. 2, p. 262–270, 2014.

ZHU, Yihua; WU, Qiufang. Synthesis of magnetite nanoparticles by precipitation with forced mixing. **Journal of Nanoparticle Research**, [s. l.], v. 1, n. 3, p. 393–396, 1999.

APENDIX A – Encapsulation of 4-nitrochalcone via miniemulsion polymerization

1 MATERIALS AND METHODS

1.1 Materials

The renewable monomer and the encapsulation of 4NC and MNPs in PTEe were made with 10-undecenoic acid (Sigma-Aldrich, 98%), 1,3-propanediol (Sigma-Aldrich, 99.6%), p-toluenesulfonic acid monohydrate (Sigma-Aldrich, 98.5%), sodium dodecyl sulfate (SDS, Vetec), azobisisobutyronitrile (AIBN, Vetec, 98%), potassium persulfate (KPS, Vetec, 99%), 1,4-butanedithiol (Sigma-Aldrich, >97%) and 4-nitrochalcone (4NC, Sigma-Aldrich). Sodium phosphate monobasic (NaH_2PO_4) and sodium phosphate dibasic (Na_2HPO_4), purchased from Vetec, were used as buffers for the *in vitro* assayss. Distilled water was used throughout the experiments.

1.2 Encapsulation of 4NC via miniemulsion polymerization

4NC-PTEe nanoparticles were prepared by thiol-ene polymerization in miniemulsion. The aqueous phase was prepared with distilled water and 0.019 wt. % of SDS as surfactant. This phase was magnetically stirred until complete surfactant solubilization. The organic phase contained 1 g (2.45 mmol) of 1,3-propylene diundec-10-enoate (Pd10e), 0.29 mL (2.45 mmol) of 1,4-butanedithiol (BDT), 1 mol % (relative to BDT) of organic-soluble initiator (AIBN) and 1 wt. % of 4NC. The Pd10e, AIBN and 4NC were magnetically stirred until complete solubilization of the initiator and the drug. The aqueous phase was added to the organic phase and stirred for 10 min at 500 rpm. Then, BDT was added and stirred for 5 min at 250 rpm, obtaining a macroemulsion. Finally, this macroemulsion was sonicated (Fisher Scientific Sonic Dismembrator model 500 and a 1/2" tip) for 2 min (10 s on and 2 s off) in ice bath at 60% of amplitude. The final miniemulsion underwent polymerization at 80 °C for 4 h in a thermostatic bath.

1.3 Characterization

Particle size, polydispersity index, surface charge and chemical characterization of the nanoparticles were performed following the procedure described in Chapter 3, session 3.3.5. The molecular weight distributions were obtained through gel permeation chromatography using a high-performance liquid chromatography equipment (HPLC, model LC 20-A, Shimadzu) and Shim Pack GPC800 Series columns (GPC 801, GPC 804 e GPC 807), also from Shimadzu. THF was used as eluent with volumetric flow rate of 1 mL·min^{-1} at 40 °C. The GPC system was calibrated using polystyrene standards with molecular weight ranging from 580 to 9.225·106 g·mol^{-1}.

1.4 *In vitro* 4NC release profile

The *in vitro* release profile method was already described in Chapter 4, session 4.2.5.

2 RESULTS

2.1 Nanoparticles characterization

Table 1 shows the mean diameter (Dp), polydispersity index (PdI) and zeta potential obtained by DLS, besides the encapsulation efficiency (EE%) of 4NC. It is important to notice that these parameters did not suffer great impact with the change of the encapsulation method. In this case, samples exhibited Dp between 114 and 143 nm approximately, with low polydispersity indexes. The zeta potential values obtained were lower than −40 mV at physiological pH, indicating good stability without formation of aggregates, which contributes to a higher colloidal stability. The negative charges presented in the nanoparticles analyzed are associated with the presence of surfactants (SDS) adsorbed on the nanoparticles surface. Free 4NC and 4NC simultaneously encapsulated in PTEe nanoparticles have similar spectroscopy behavior, with maximum wavelength at 324 nm. The 4NC was encapsulated *in situ* and presented an encapsulation efficiency of almost 100 %.

Table 1. Intensity mean diameter of nanoparticles (Dp); polydispersity index (PdI); zeta potential in pH 7 and encapsulation efficiency (EE%).

Sample	Dp (nm)	PdI	Zeta Potential (mV)	EE (%)
blank PTEe	143 ± 4	0.20 ± 0.03	− 42 ± 3	-
4NC+PTEe	114 ± 1	0.14 ± 0.01	− 41 ± 0	99.8 ± 0.1

± Mean Standard deviation of n = 3 determinations
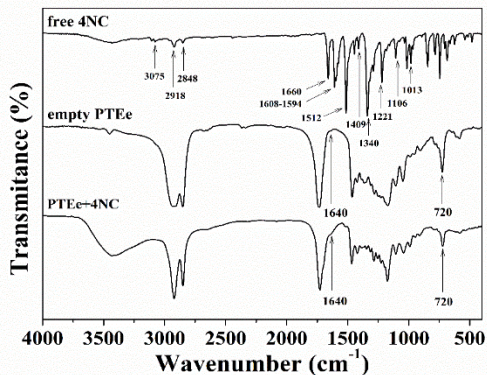Source: From the author.

Table 2 shows the number average molecular weight (Mn) and weight average molecular weight (Mw) of blank PTEe and PTEe+4NC, both obtained by miniemulsion polymerization. The values of the blank PTEe were taken from Cardoso et al. (2017). It is possible to observe that both Mn and Mw decreased with the encapsulation of 4NC.

Table 2. Intensity mean diameter of nanoparticles (Dp); polydispersity index (PdI); zeta potential in pH 7 and encapsulation efficiency (EE%).

Sample	Mn (kDa)	Mw (kDa)
blank PTEe	15.3	33.9
4NC+PTEe	3.9	6.6

Source: From the author.

The presence of the absorption bands of the functional groups present in the samples could be verified by FT-IR analyses, which are displayed in Figure 1. The results were very similar to the ones observed at the previous chapters. As in the previous analyses, it was possible to identify the main bands corresponding to the polymer. Again, the comparison between the FT-IR spectra of MNPs+4NC PTEe and free 4NC suggests that there is no significant interaction between the drug and the polymer, showing that 4NC is located in the polymeric matrix (molecularly dispersed) and not at the surface.

Figure 1. FTIR analyses of the free 4NC and PTEe nanoparticles.

Source: From the author.

3.2 *In vitro* release profile

The *in vitro* release study was performed in order to evaluate the release profile of 4NC encapsulated in PTEe via miniemulsion polymerization. In this case, the amount of 4NC released from the PTEe NPs reached 70% after the first 24 h and 95% after 6 days in the medium with pH 7.4. This result is displayed in Figure 2. The release was faster compared to the MNPs+4NC-PTEe nanoparticles synthesized by miniemulsification and solvent evaporation method and could be explained with the decrease in molecular weight. It is important to mention that the dashed lines indicate only the profile's tendency, and do not represent any mathematical model applied on the experimental data.

The zero order, first order, Higuchi and Korsmeyer-Peppas mathematical models were evaluated and the choice of the best model was made by linear correlation (R^2). The Higuchi model presented the highest value of R^2, as it can be seen in Table 2. This model is based on Fick's first law, whereby the release occurs by the diffusion of the drug within the delivery system. Therefore, this result suggests that the release of 4NC from nanoparticles synthesized by miniemulsion polymerization is also controlled by diffusion.

Figure 2. Release profile of 4NC loaded in PTEe nanoparticles in pH 7.4.
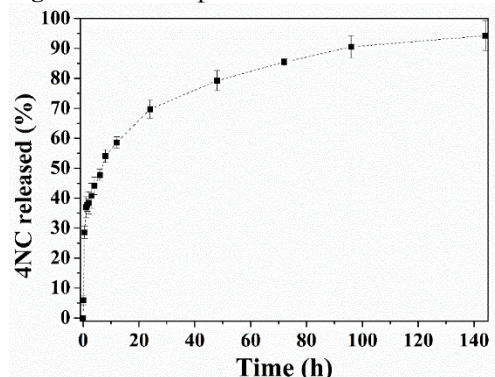
Source: From the author.

Table 2. Mathematical models utilized to evaluate the 4NC release profile and R^2 values for pH 7.4.

Mathematical models	Equation	R^2
Zero order	$Q_t = Q_0 + K_0 t$	0.712
First order	$lnQ_t = lnQ_0 + K_1 t$	0.360
Higuchi	$Q_t/Q_\infty = K_k t^n$	0.895
Korsmeyer-Peppas	$Q_t = K_H \sqrt{t}$	0.599

Source: From the author.

4 CONCLUSION

Using miniemulsion polymerization, the 4NC was successfully encapsulated, obtaining an EE% greater than 99%, with good Dp, PdI and zeta potential values. The 4NC release profile was obtained for pH 7.4, occurring also through diffusion. The release was faster than the MNPs+4NC-PTEe synthesized by miniemulsification and solvent evaporation, which could be explained by the decrease observed in the molecular weight. This method presented the advantage of being able to incorporate 4NC in only one step and without using organic solvents. Although more assays are necessary to prove its effectiveness, the synthesized materials demonstrated potential to be used in biomedical applications such as cancer treatment.